AFOSR Scientific Report AFOSR 65-0640
ASRL TR 112-4

VIBRATIONS OF FREELY-SUPPORTED ORTHOTROPIC CYLINDRICAL SHELLS UNDER INTERNAL PRESSURE

Peter R. DiGiovanni
John Dugundji

MASSACHUSETTS INSTITUTE OF TECHNOLOGY
AEROELASTIC AND STRUCTURES RESEARCH LABORATORY

February 1965

AIR FORCE OFFICE OF SCIENTIFIC RESEARCH
UNITED STATES AIR FORCE
GRANT NO. AFOSR-62-363

AFOSR Scientific Report AFOSR 65-0640
ASRL TR 112-4

VIBRATIONS OF FREELY-SUPPORTED ORTHOTROPIC CYLINDRICAL SHELLS UNDER INTERNAL PRESSURE

Peter R. DiGiovanni
John Dugundji

MASSACHUSETTS INSTITUTE OF TECHNOLOGY
AEROELASTIC AND STRUCTURES RESEARCH LABORATORY

February 1965

AIR FORCE OFFICE OF SCIENTIFIC RESEARCH
UNITED STATES AIR FORCE
GRANT NO. AFOSR-62-363

FOREWORD

This report was made within the Aeroelastic and Structures Research Laboratory under United States Air Force Grant No. AF OSR-62-363. The project is administered by Dr. J. Pomerantz of the Air Force Office of Scientific Research, United States Air Force.

ABSTRACT

The influence of orthotropicity and internal pressure on the natural frequencies of a thin cylindrical shell whose ends are freely supported is found using the shell equations of Washizu. Other common shell theories are also presented.

Calculations are performed for four constant thickness orthotropic cylinders, two stiffened cylinders, and a basic isotropic cylinder. For these calculations, only the special cases of axial and circumferential stiffening were considered.

It is noted that there is a difference in the behavior of the frequencies for the $n = 0$, $n = 1$, and $n \geq 2$ modes. For the $n \geq 2$ modes, the lowest frequency is associated with predominantly radial motion. For the $n = 0$ mode, the lowest frequency is either associated with uncoupled torsional motion or predominantly radial motion, depending on the axial wave length. For the $n = 1$ mode, the lowest frequency is associated with a combination of circumferential and radial motion.

For the $n \geq 2$ and $n = 0$ modes, circumferential stiffening generally increased significantly the frequency of the predominantly radial mode, while axial stiffening had little effect on these frequencies. For the $n = 1$ beam-type mode, axial stiffening increased the frequency, while circumferential stiffening has little effect on the frequency.

Internal pressure significantly increased the frequency of the predominantly radial mode for all cases of stiffening for $n \geq 2$, while there was little effect on the $n = 0$ mode. Internal pressure had small effect on the $n = 1$ beam-type mode for all cases of stiffening.

TABLE OF CONTENTS

LIST OF SYMBOLS

b_{ij}	Elastic stiffnesses referred to x-y axes
C_{ij}	Stretching stiffnesses referred to x-y axes
D_{ij}	Bending and twisting stiffnesses referred to x-y axes
D_s	Bending stiffness of unstiffened shell, $Et_s^3/(1-\nu^2)$
E	Modulus of elasticity
F_1, F_2, F_3	Defined in Table 1
F_x, F_θ, F_z	Forces per unit area in axial, circumferential, and radial directions
G	Shear modulus
G_1, G_2, G_3	Defined in Table 2
h	Thickness of orthotropic material
ℓ	Length of cylinder
m	Longitudinal mode number, number of axial half-waves
m*	Mass per unit area of cylinder
$M_x, M_\theta, M_{x\theta}$	Moment resultants per unit length
n	Circumferential mode number, number of circumferential waves
$N_x, N_\theta, N_{x\theta}$	Force resultants per unit length
$\bar{N}_x, \bar{N}_\theta$	Initial force resultants
$\bar{n}_x$	Dimensionless initial axial force, $\bar{N}_x/C'_{22}$
$\bar{n}_\theta$	Dimensionless initial circumferential force, $\bar{N}_\theta/C'_{22}$

p	Internal pressure
R	Radius of cylinder
t	Time
u,v,w	Axial, circumferential, and radial displacements of cylinder mid-surface
$\bar{u},\bar{v},\bar{w}$	Initial axial, circumferential, and radial displacements of cylinder mid-surface
u_{mn},v_{mn},w_{mn}	Magnitudes of displacements associated with mn mode
β	$(1/12)(D'_{22}/C'_{22})$
δ	Variational notation
Ω	Dimensionless frequency stiffness parameter, $R\omega\sqrt{m^*/C'_{22}}$
$\epsilon_x,\epsilon_\theta,\gamma_{x\theta}$	Strain components
$\epsilon_{x_o},\epsilon_{\theta_o},\gamma_{x\theta_o}$	Mid-surface strains
θ	Angular coordinate
$\kappa_x,\kappa_\theta,\kappa_{x\theta}$	Curvature strains
λ	Axial wave-length factor, $m\pi R/\ell$
ν	Poisson's ratio
ρ	Density
$\sigma_x,\sigma_\theta,\sigma_{x\theta}$	Stress components
φ	Angle between geometric and principal elastic axis
ω	Circular frequency

Subscripts

s	Pertaining to skin
w	Pertaining to web

Superscripts

( )'	Referred to principal elastic axes

1. INTRODUCTION

Many papers have been written on the free vibrations of a thin circular cylindrical shell. For example, Arnold and Warburton (Ref. 1) have investigated the frequency spectrum for freely-supported circular cylindrical shells using a set of displacement equations of motion which are similar to those of Goldenveizer (Ref. 2).

The effect of initial circumferential and axial stresses on the vibration frequencies of freely-supported isotropic cylindrical shells has been studied by Reissner (Refs. 3, 4). In Ref. 3,he derived a simple expression for the frequency on the basis of Maguerre's shallow-shell theory by omitting the effect of circumferential and longitudinal inertia terms. The results obtained in Ref. 3 cannot be expected to be valid for modes having a small circumferential wave number, due to the shallow-shell approximation. In Ref. 4, Reissner developed the frequency equation for isotropic cylindrical shells using membrane theory, including all inertia effects.

Fung, Sechler and Kaplan (Ref. 5) have also studied the effect of pressure on the vibration frequencies of freely-supported cylindrical shells. To include the effect of pressure, the nonlinear equations of Timoshenko (Ref. 6) are used. However, the calculations were carried out using the frequency equation of Reissner (Ref. 3).

More recently, Armenákas (Ref. 7) has investigated the effect of initial stress on simply-supported isotropic cylindrical shells using a shell theory developed by Herrmann and Armenákas (Ref. 8) which includes the effect on the motion of the change due to deformation of the magnitude and direction of the applied

initial load.

This investigation is primarily concerned with the effect of circumferential and axial stiffening, as well as internal pressure on the frequencies and mode shapes, of a freely-supported cylinder.

2. BASIC SHELL EQUATIONS AND RELATIONS

Shown in Fig. 1a is the middle surface of an orthotropic cylindrical shell. The x-y axes are the geometric axes, while the x'-y' are the principal axes rotated an angle φ with respect to the geometric axes. The stiffened axis of the cylinder will be taken as x'. The stress resultants and couples are shown in Fig. 1b.

The boundary conditions used here are those called freely-supported by Arnold and Warburton (Ref. 1) and are given by

$$\begin{aligned} v(0,\theta,t) &= v(\ell,\theta,t) = 0 \\ w(0,\theta,t) &= w(\ell,\theta,t) = 0 \\ N_x(0,\theta,t) &= N_x(\ell,\theta,t) = 0 \\ M_x(0,\theta,t) &= M_x(\ell,\theta,t) = 0 \end{aligned} \tag{1}$$

The effect of other boundary conditions on the modal characteristics of thin isotropic cylindrical shells has been investigated in detail by Forsberg (Ref. 9).

2.1 Thin Cylindrical Shell Equations using Washizu's Shell Theory

From Fig. 1, assuming that the thickness is small compared to the radius (we limit ourselves here to Love's first approximation, i.e., $1 + z/R \sim 1$), the stress resultants are

$$N_x = \int_{-h/2}^{h/2} \sigma_x \, dz \tag{2}$$

$$N_\theta = \int_{-h/2}^{h/2} \sigma_\theta \, dz \tag{3}$$

$$N_{x\theta} = N_{\theta x} = \int_{-h/2}^{h/2} \sigma_{x\theta} \, dz \tag{4}$$

and the stress couples by

$$M_x = \int_{-h/2}^{h/2} \sigma_x \, z \, dz \tag{5}$$

$$M_\theta = \int_{-h/2}^{h/2} \sigma_\theta \, z \, dz \tag{6}$$

$$M_{x\theta} = M_{\theta x} = \int_{-h/2}^{h/2} \sigma_{x\theta} \, z \, dz \tag{7}$$

Strain-Displacement Relations

The effect of transverse shear is neglected and normal strains are assumed to be zero. When the Euler-Bernoulli-Navier hypothesis is also employed, the strains can be written as

$$\epsilon_x = \epsilon_{x_o} - z\kappa_x \tag{8}$$

$$\epsilon_\theta = \epsilon_{\theta_o} - z\kappa_\theta \tag{9}$$

$$\gamma_{x\theta} = \gamma_{x\theta_o} - 2z\kappa_{x\theta} \tag{10}$$

where ϵ_{x_o}, ϵ_{θ_o}, and $\gamma_{x\theta_o}$ are the mid-surface strains and κ_x, κ_θ, and $\kappa_{x\theta}$ are the curvature strains.

Using what Washizu (Ref. 10) calls the thin shell of Type D, the strains are related to the mid-surface displacements by

$$\epsilon_{x_o} = \frac{\partial u}{\partial x} + \frac{1}{2}\left[\left(\frac{\partial u}{\partial x}\right)^2 + \left(\frac{\partial v}{\partial x}\right)^2 + \left(\frac{\partial w}{\partial x}\right)^2\right] \tag{11}$$

$$\epsilon_{\theta_o} = \frac{1}{R}\frac{\partial v}{\partial \theta} - \frac{w}{R} + \frac{1}{2R^2}\left[\left(\frac{\partial u}{\partial \theta}\right)^2 + \left(\frac{\partial v}{\partial \theta} - w\right)^2 + \left(\frac{\partial w}{\partial \theta} + v\right)^2\right] \tag{12}$$

$$\gamma_{x\theta_o} = \frac{\partial v}{\partial x} + \frac{1}{R}\frac{\partial u}{\partial \theta} + \frac{1}{R}\left[\frac{\partial u}{\partial x}\frac{\partial u}{\partial \theta} + \frac{\partial v}{\partial x}\left(\frac{\partial v}{\partial \theta} - w\right) + \frac{\partial w}{\partial x}\left(\frac{\partial w}{\partial \theta} + v\right)\right] \tag{13}$$

$$K_x = \frac{\partial^2 w}{\partial x^2} \tag{14}$$

$$K_\theta = \frac{1}{R^2}\left(\frac{\partial^2 w}{\partial \theta^2} + \frac{\partial v}{\partial \theta}\right) \tag{15}$$

$$K_{x\theta} = \frac{1}{R}\left(\frac{\partial^2 w}{\partial x \partial \theta} + \frac{\partial v}{\partial x}\right) \tag{16}$$

These expressions include nonlinear terms in midplane strains, but not in the curvature strains.*

Stress-Strain Relations

The stress-strain relations for a thin orthotropic cylindrical shell are

$$N_x = C_{11}\epsilon_{x_o} + C_{12}\epsilon_{\theta_o} + C_{13}\gamma_{x\theta_o} \tag{17}$$

$$N_\theta = C_{12}\epsilon_{x_o} + C_{22}\epsilon_{\theta_o} + C_{23}\gamma_{x\theta_o} \tag{18}$$

$$N_{x\theta} = C_{13}\epsilon_{x_o} + C_{23}\epsilon_{\theta_o} + C_{33}\gamma_{x\theta_o} \tag{19}$$

$$M_x = -\left(D_{11}K_x + D_{12}K_\theta + 2D_{13}K_{x\theta}\right) \tag{20}$$

$$M_\theta = -\left(D_{12}K_x + D_{22}K_\theta + 2D_{23}K_{x\theta}\right) \tag{21}$$

*The nonlinear terms in the curvature strains are omitted here since they will offer no contribution to the final linearized cylindrical shell equations under initial membrane stresses.

$$M_{x\theta} = -\left(D_{13}\kappa_x + D_{23}\kappa_\theta + 2D_{33}\kappa_{x\theta}\right) \tag{22}$$

Equations of Equilibrium

For the special case of the boundary conditions given in Eqs. (1), the principle of virtual work as applied to the cylindrical shell can be written as

$$\iint_S \Big(N_x\,\delta\epsilon_{x_0} + N_\theta\,\delta\epsilon_{\theta_0} + N_{x\theta}\,\delta\gamma_{x\theta_0} - M_x\,\delta\kappa_x - M_\theta\,\delta\kappa_\theta - 2M_{x\theta}\,\delta\kappa_{x\theta}\Big)R\,dx\,d\theta - \iint_S \Big(F_x\,\delta u + F_\theta\,\delta v + F_z\,\delta w\Big)R\,dx\,d\theta = 0 \tag{23}$$

where S is the area of the mid-surface and F_x, F_θ, and F_z are the body forces per unit of mid-surface area. The equilibrium equations obtained from Eq. (23) depend on the strain-displacement relations given by Eqs. (11) through (16). This leads to the following nonlinear equilibrium equations of Washizu (Refs. 10 and 11).

$$\frac{\partial}{\partial x}\left[N_x R\left(1+\frac{\partial u}{\partial x}\right) + N_{\theta x}\frac{\partial u}{\partial \theta}\right] + \frac{\partial}{\partial \theta}\left[\frac{N_\theta}{R}\frac{\partial u}{\partial \theta} + N_{\theta x}\left(1+\frac{\partial u}{\partial x}\right)\right] + F_x R = 0 \tag{24}$$

$$\frac{\partial}{\partial x}\left[N_x R \frac{\partial v}{\partial x} + N_{x\theta} R\left(1 + \frac{1}{R}\frac{\partial v}{\partial \theta} - \frac{w}{R}\right)\right]$$

$$+ \frac{\partial}{\partial \theta}\left[N_\theta\left(1 + \frac{1}{R}\frac{\partial v}{\partial \theta} - \frac{w}{R}\right) + N_{x\theta}\frac{\partial v}{\partial x}\right] - \left[N_\theta\left(\frac{v}{R} + \frac{1}{R}\frac{\partial w}{\partial \theta}\right)\right.$$

$$\left. + N_{x\theta}\frac{\partial w}{\partial x}\right] - \frac{1}{R}\left(\frac{\partial M_\theta}{\partial \theta} + 2R\frac{\partial M_{x\theta}}{\partial x}\right) + F_\theta R = 0 \qquad (25)$$

$$\frac{\partial}{\partial x}\left[N_x R \frac{\partial w}{\partial x} + N_{x\theta}\left(v + \frac{\partial w}{\partial \theta}\right)\right] + \frac{\partial}{\partial \theta}\left[N_\theta\left(\frac{v}{R} + \frac{1}{R}\frac{\partial w}{\partial \theta}\right)\right.$$

$$\left. + N_{x\theta}\frac{\partial w}{\partial x}\right] + N_\theta\left(1 + \frac{1}{R}\frac{\partial v}{\partial \theta} - \frac{w}{R}\right) + N_{x\theta}\frac{\partial v}{\partial x}$$

$$+ \frac{\partial}{\partial x}\left[R\frac{\partial M_x}{\partial x} + \frac{\partial M_{x\theta}}{\partial \theta}\right] + \frac{\partial}{\partial \theta}\left[\frac{1}{R}\frac{\partial M_\theta}{\partial \theta} + \frac{\partial M_{x\theta}}{\partial x}\right] + F_z R = 0 \qquad (26)$$

2.2 The Frequency Equation

For the vibration problem, the nonlinear equilibrium equations [Eqs. (24) through (26)] are used as a basis for deriving the influence of internal pressure on the frequencies and mode shapes of the thin cylindrical shell. The shell stresses and displacements can be expressed in terms of deviations from an initially stressed configuration. We take here the case where

the only initial stress resultants are $\bar{N}_x$ and $\bar{N}_\theta$, and all the initial stress couples are zero. That is, let

$$N_x = \bar{N}_x + \tilde{N}_x$$

$$N_\theta = \bar{N}_\theta + \tilde{N}_\theta \qquad (27)$$

$$N_{x\theta} = \tilde{N}_{x\theta}$$

$$M_x = \tilde{M}_x \,, \qquad M_\theta = \tilde{M}_\theta \,, \qquad M_{x\theta} = \tilde{M}_{x\theta} \qquad (28)$$

and

$$u = \bar{u} + \tilde{u} \,, \qquad v = \bar{v} + \tilde{v} \,, \qquad w = \bar{w} + \tilde{w} \qquad (29)$$

where $\bar{N}_x$, $\bar{N}_\theta$, $\bar{u}$, $\bar{v}$, and $\bar{w}$ are those stress resultants and displacements resulting from the static loading conditions and $\tilde{N}_x$, $\tilde{N}_\theta$, $\tilde{N}_{x\theta}$, $\tilde{M}_x$, $\tilde{M}_\theta$, $\tilde{M}_{x\theta}$, $\tilde{u}$, $\tilde{v}$, and $\tilde{w}$ are the vibratory stress resultants, couples, and displacements.

Considered in this report is the case in which the internal pressure is taken as Constant Directional, i.e., the direction and magnitude per unit original area remains unchanged during deformation. For a consideration of the case where the direction and magnitude per unit original area changes with deformation due to the internal pressure, see Ref. 8.*

All the vibratory stress resultants and couples, as well as the vibratory displacements, are considered infinitesimal quantities for the vibration problem and it is justifiable to neglect their squares and products. It is also assumed that $\bar{N}_x$ and $\bar{N}_\theta$ are constant and

*For that case, additional terms $p\,\frac{\partial w}{\partial x}$, $\frac{p}{R}\left(\frac{\partial w}{\partial \theta} + v\right)$, and $-p\left[\frac{\partial u}{\partial x} + \frac{1}{R}\left(\frac{\partial v}{\partial \theta} - \frac{w}{R}\right)\right]$ would be added to the left-hand sides of Eqs. (31), (32), and (33), respectively.

$$F_x = -m^* \frac{\partial^2 u}{\partial t^2}, \quad F_\theta = -m^* \frac{\partial^2 v}{\partial t^2}, \quad F_z = -m^* \frac{\partial^2 w}{\partial t^2} \tag{30}$$

With this simplification Eqs. (24) through (26) become (here, for convenience of notation we now write the vibratory stresses and displacements $\tilde{N}_x$, $\tilde{N}_\theta$, $\tilde{u}$, $\tilde{v}$, and $\tilde{w}$, as N_x, N_θ, u, v, and w).

$$\frac{\partial N_x}{\partial x} + \frac{1}{R}\frac{\partial N_{x\theta}}{\partial \theta} + \bar{N}_x \frac{\partial^2 u}{\partial x^2} + \frac{\bar{N}_\theta}{R^2}\frac{\partial^2 u}{\partial \theta^2} - m^* \frac{\partial^2 u}{\partial t^2} = 0 \tag{31}$$

$$\frac{\partial N_{x\theta}}{\partial x} + \frac{1}{R}\frac{\partial N_\theta}{\partial \theta} - \frac{1}{R^2}\left(\frac{\partial M_\theta}{\partial \theta} + 2R\frac{\partial M_{x\theta}}{\partial x}\right) + \bar{N}_x \frac{\partial^2 v}{\partial x^2}$$

$$+ \frac{\bar{N}_\theta}{R}\left(\frac{\partial^2 v}{\partial \theta^2} - \frac{\partial w}{\partial \theta}\right) - \frac{\bar{N}_\theta}{R^2}\left(v + \frac{\partial w}{\partial \theta}\right) - m^* \frac{\partial^2 v}{\partial t^2} = 0 \tag{32}$$

$$\frac{N_\theta}{R} + \frac{\partial^2 M_x}{\partial x^2} + \frac{2}{R}\frac{\partial^2 M_{x\theta}}{\partial x \partial \theta} + \frac{1}{R^2}\frac{\partial M_\theta}{\partial \theta^2} + \bar{N}_x \frac{\partial^2 w}{\partial x^2}$$

$$+ \frac{\bar{N}_\theta}{R^2}\left(\frac{\partial v}{\partial \theta} + \frac{\partial^2 w}{\partial \theta^2}\right) + \frac{\bar{N}_\theta}{R^2}\left(\frac{\partial v}{\partial \theta} - w\right) - m^* \frac{\partial^2 w}{\partial t^2} = 0 \tag{33}$$

where Eqs. (31) through (33) represent the equilibrium equations of free vibration of a thin cylindrical shell about an initially stressed configuration.

By combining Eqs. (11) through (16) and Eqs. (17) through (22) and substituting this result into Eqs. (31) through (33), the following differential equations in u, v, and w are obtained.

$$\frac{C_{11}}{C'_{22}}\frac{\partial^2 u}{\partial x^2}+\frac{2}{R}\frac{C_{13}}{C'_{22}}\frac{\partial^2 u}{\partial x\partial\theta}+\frac{1}{R^2}\frac{C_{33}}{C'_{22}}\frac{\partial^2 u}{\partial\theta^2}+\frac{C_{13}}{C'_{22}}\frac{\partial^2 v}{\partial x^2}$$

$$+\frac{1}{R}\frac{C_{12}+C_{33}}{C'_{22}}\frac{\partial^2 v}{\partial x\partial\theta}+\frac{1}{R^2}\frac{C_{23}}{C'_{22}}\frac{\partial^2 v}{\partial\theta^2}-\frac{1}{R}\frac{C_{12}}{C'_{22}}\frac{\partial w}{\partial x}$$

$$-\frac{1}{R^2}\frac{C_{23}}{C'_{22}}\frac{\partial w}{\partial\theta}+\frac{1}{R^2}\frac{D'_{22}}{C'_{22}}F_1(u,v,w)+G_1(\bar{N}_x,\bar{N}_\theta,u,v,w)$$

$$-\frac{m^*}{C'_{22}}\frac{\partial^2 u}{\partial t^2}=0 \qquad (34)$$

$$\frac{C_{13}}{C'_{22}}\frac{\partial^2 u}{\partial x^2}+\frac{1}{R}\frac{C_{12}+C_{33}}{C'_{22}}\frac{\partial^2 u}{\partial x\partial\theta}+\frac{1}{R^2}\frac{C_{23}}{C'_{22}}\frac{\partial^2 u}{\partial\theta^2}+\frac{C_{33}}{C'_{22}}\frac{\partial^2 v}{\partial x^2}$$

$$+\frac{2}{R}\frac{C_{23}}{C'_{22}}\frac{\partial^2 v}{\partial x\partial\theta}+\frac{1}{R^2}\frac{C_{22}}{C'_{22}}\frac{\partial^2 v}{\partial\theta^2}-\frac{1}{R^2}\frac{C_{23}}{C'_{22}}\frac{\partial w}{\partial x}-\frac{1}{R^2}\frac{C_{22}}{C'_{22}}\frac{\partial w}{\partial\theta}$$

$$+\frac{1}{R^2}\frac{D'_{22}}{C'_{22}}F_2(u,v,w)+G_2(\bar{N}_x,\bar{N}_\theta,u,v,w)$$

$$-\frac{m^*}{C'_{22}}\frac{\partial^2 v}{\partial t^2}=0 \qquad (35)$$

$$\frac{1}{R}\frac{C_{12}}{C'_{22}}\frac{\partial u}{\partial x}+\frac{1}{R^2}\frac{C_{23}}{C'_{22}}\frac{\partial u}{\partial \theta}+\frac{1}{R}\frac{C_{23}}{C'_{22}}\frac{\partial v}{\partial x}+\frac{1}{R^2}\frac{C_{22}}{C'_{22}}\frac{\partial v}{\partial \theta}$$

$$-\frac{1}{R^2}\frac{C_{22}}{C'_{22}}w-\frac{1}{R^2}\frac{D'_{22}}{C'_{22}}\left[\frac{D_{11}}{D'_{22}}R^2\frac{\partial^4 w}{\partial x^4}+2\frac{D_{12}+2D_{33}}{D'_{22}}\frac{\partial^4 w}{\partial x^2\partial\theta^2}\right.$$

$$\left.+\frac{1}{R^2}\frac{D_{22}}{D'_{22}}\frac{\partial^4 w}{\partial\theta^4}\right]+\frac{1}{R^2}\frac{D'_{22}}{C'_{22}}F_3(u,v,w)+G_3(\bar{N}_x,\bar{N}_\theta,u,v,w) \qquad (36)$$

$$-\frac{m^*}{C'_{22}}\frac{\partial^2 w}{\partial t^2}=0$$

The expressions for F_1, F_2, F_3, and G_1, G_2, G_3 appearing in Eqs. (34) through (36) are given in Table 1. The explicit values of F_1, F_2, F_3 used here are those of Washizu (Ref. 10), Novozhilov (Ref. 16), and Goldenviezer (Ref. 2), while the G_1, G_2, G_3 are those of Washizu (Ref. 10) and Herrmann (Ref. 8).

Numerous other versions of the cylindrical shell equations have been published in the literature. All of these versions may be written in the form of Eqs. (34) through (36) in which minor differences are reflected in the functions F_1, F_2, F_3, and G_1, G_2, G_3. Some other common theories are also listed in Table 1.

We will be concerned in what follows with the special cases of orthotropicity where the geometric and principal axes are parallel and perpendicular, i.e., $\varphi = 0$ and 90 degrees. This corresponds to the conditions

$$\frac{C_{13}}{C'_{22}}=\frac{C_{23}}{C'_{22}}=\frac{D_{13}}{D'_{22}}=\frac{D_{23}}{D'_{22}}=0 \qquad (37)$$

With this simplification, a solution to Eqs. (34) through (36) which satisfies the boundary conditions [Eq. (1)] is

$$u = u_{mn} \cos\frac{m\pi x}{\ell} \cos n\theta\, e^{i\omega t}$$

$$v = v_{mn} \sin\frac{m\pi x}{\ell} \sin n\theta\, e^{i\omega t} \qquad (38)$$

$$w = w_{mn} \sin\frac{m\pi x}{\ell} \cos n\theta\, e^{i\omega t}$$

where m and n are integers and w is the natural frequency of vibration. The integer n represents the number of circumferential waves, while the integer m, the number of axial half waves. A pair of integers m, n then specifies a particular mode shape.

Upon substituting Eqs. (38) into Eqs. (34) through (36) there are obtained three homogeneous linear algebraic equations in u_{mn}, v_{mn}, and w_{mn}, the nontrivial solution of which requires

$$
\begin{vmatrix}
\dfrac{C_{11}}{C'_{22}}\lambda^2 + \dfrac{C_{33}}{C'_{22}}\eta^2 + \bar{n}_x\lambda^2 & -\dfrac{C_{12}+C_{33}}{C'_{22}}\lambda\eta & \dfrac{C_{12}}{C'_{22}}\lambda \\
\bar{n}_0\eta^2 - \Omega^2 & & \\
-\dfrac{C_{12}+C_{33}}{C'_{22}}\lambda\eta & \dfrac{C_{33}}{C'_{22}}\lambda^2 + \dfrac{C_{22}}{C'_{22}}\eta^2 + \beta\left\{\dfrac{D_{22}}{D'_{22}}\eta^2 + 4\dfrac{D_{33}}{D'_{22}}\lambda^2\right\} + \bar{n}_0(\eta^2+1) & -\eta\left(\dfrac{C_{22}}{C'_{22}} + \beta\left\{\dfrac{D_{22}}{D'_{22}}\eta^2 + \dfrac{D_{12}+4D_{33}}{D'_{22}}\lambda^2\right\} + 2\bar{n}_0\right) \\
 & + \bar{n}_x\lambda^2 - \Omega^2 & \\
\dfrac{C_{12}}{C'_{22}}\lambda & -\eta\left(\dfrac{C_{22}}{C'_{22}} + \beta\left\{\dfrac{D_{22}}{D'_{22}}\eta^2 + \dfrac{D_{12}+4D_{33}}{D'_{22}}\lambda^2\right\} + 2\bar{n}_0\right) & \dfrac{C_{22}}{C'_{22}} + \beta\left\{\dfrac{D_{11}}{D'_{22}}\lambda^4 + 2\dfrac{D_{12}+4D_{33}}{D'_{22}}\eta^2\lambda^2 + \dfrac{D_{22}}{D'_{22}}\eta^4\right\} + \bar{n}_x\lambda^2 + \bar{n}_0(\eta^2+1) - \Omega^2
\end{vmatrix} = 0 \qquad (39)
$$

where

$$\Omega = R\omega\sqrt{\rho m^2/C_{22}'} \qquad \lambda = \frac{m\pi R}{\ell}$$

$$\bar{n}_x = \frac{\bar{N}_x}{C_{22}'} \qquad \bar{n}_\theta = \frac{\bar{N}_\theta}{C_{22}'} \tag{40}$$

Note that the vibration frequency and initial stresses are referenced with respect to C_{22}', i.e., the stretching stiffness along the unstiffened y' direction.

When $\bar{n}_x$ and $\bar{n}_\theta$ vanish and the material is isotropic, Eq. (39) reduces to that given by Arnold and Warburton (Ref. 1). If the determinant is written as

$$\begin{vmatrix} a_{11} - \Omega^2 & a_{12} & a_{13} \\ a_{21} & a_{22} - \Omega^2 & a_{23} \\ a_{31} & a_{32} & a_{33} - \Omega^2 \end{vmatrix} = 0 \tag{41}$$

there is provided a frequency equation of the form

$$\Omega^6 - K_2\Omega^4 + K_1\Omega^2 - K_0 = 0 \tag{42}$$

where

$$K_2 = a_{11} + a_{22} + a_{33}$$

$$K_1 = \begin{vmatrix} a_{11} & a_{12} \\ a_{21} & a_{22} \end{vmatrix} + \begin{vmatrix} a_{11} & a_{13} \\ a_{31} & a_{33} \end{vmatrix} + \begin{vmatrix} a_{22} & a_{23} \\ a_{32} & a_{33} \end{vmatrix} \tag{43}$$

$$K_o = \begin{vmatrix} a_{11} & a_{12} & a_{13} \\ a_{21} & a_{22} & a_{23} \\ a_{31} & a_{32} & a_{33} \end{vmatrix}$$

Associated with the three positive roots ($\Omega_1 < \Omega_2 < \Omega_3$) of Eq. (42) are three mode shapes given by

$$\frac{U_{mn}}{W_{mn}} = -\frac{N_u}{D}$$
$$\frac{V_{mn}}{W_{mn}} = -\frac{N_v}{D} \qquad (44)$$

where

$$D = \begin{vmatrix} a_{11} - \Omega^2 & a_{12} \\ a_{21} & a_{22} - \Omega^2 \end{vmatrix}$$
$$N_u = \begin{vmatrix} a_{13} & a_{12} \\ a_{23} & a_{22} - \Omega^2 \end{vmatrix} \qquad (45)$$
$$N_v = \begin{vmatrix} a_{11} - \Omega^2 & a_{13} \\ a_{21} & a_{23} \end{vmatrix}$$

The general character of these mode shapes depends on the shell parameters and nodal pattern.

3. APPLICATION TO CONSTANT THICKNESS ORTHOTROPIC AND STIFFENED CYLINDERS

The results of the preceding section are now applied to an orthotropic cylinder of constant thickness and also to a stiffened cylinder of skin thickness t_s, which is integrally stiffened on one side (Table 4). In the latter case, it is assumed that the spacing of the stiffeners is small compared to the radius and length, so that for the purpose of studying overall or average behavior, it is plausible to replace the actual cylinder by an equivalent uniform orthotropic cylinder. Note that in this report the shell theory used applies to cross sections of shell elements which are symmetrical with respect to the middle surface. For asymmetric cross sections, there will be coupling between the mid-surface strains and changes of curvatures. This coupling effect is omitted here.

3.1 Properties of Constant Thickness Orthotropic Cylindrical Shell

For an orthotropic material of constant thickness h, it is possible to express the stress-strain law in the form

$$\begin{aligned} \sigma_x &= b_{11}\epsilon_x + b_{12}\epsilon_\theta + b_{13}\gamma_{x\theta} \\ \sigma_\theta &= b_{12}\epsilon_x + b_{22}\epsilon_\theta + b_{23}\gamma_{x\theta} \\ \sigma_{x\theta} &= b_{13}\epsilon_x + b_{23}\epsilon_\theta + b_{33}\gamma_{x\theta} \end{aligned} \tag{46}$$

where the b_{ij} are the elastic stiffnesses of the cylindrical shell referred to the x-y axes. The stiffness b_{ij} can be written in terms of the stiffnesses b'_{ij} referred to the principal axes, x'-y', as shown in Ref. 12 as follows:

$$b_{11} = b_{11}' \cos^4\phi + b_{22}' \sin^4\phi + 2\left(b_{12}' + 2b_{33}'\right)\cos^2\phi \sin^2\phi$$

$$b_{12} = \left(b_{11}' + b_{22}' - 4b_{33}'\right)\cos^2\phi \sin^2\phi + b_{12}'\left(\cos^4\phi + \sin^4\phi\right)$$

$$b_{22} = b_{11}' \sin^4\phi + b_{22}' \cos^4\phi + 2\left(b_{12}' + 2b_{33}'\right)\cos^2\phi \sin^2\phi$$

$$b_{13} = \left[b_{22}' \sin^2\phi - b_{11}' \cos^2\phi - \left(b_{12}' + 2b_{33}'\right)\left(\cos^2\phi - \sin^2\phi\right)\right]\cos\phi \sin\phi \qquad (47)$$

$$b_{23} = \left[b_{22}' \cos^2\phi - b_{11}' \sin^2\phi - \left(b_{12}' + 2b_{33}'\right)\left(\cos^2\phi - \sin^2\phi\right)\right]\cos\phi \sin\phi$$

$$b_{33} = \left(b_{11}' + b_{22}' - 2b_{12}'\right)\cos^2\phi \sin^2\phi + b_{33}'\left(\cos^2\phi - \sin^2\phi\right)^2$$

where the four independent material constants b_{ij}' have the following physical meaning

$$b_{11}' = \frac{E_{x'}}{1 - \nu_{\theta' x'} \nu_{x' \theta'}} \qquad b_{22}' = \frac{E_{\theta'}}{1 - \nu_{\theta' x'} \nu_{x' \theta}}$$

$$b_{12}' = \frac{\nu_{\theta' x'} E_{x'}}{1 - \nu_{\theta' x'} \nu_{x' \theta'}} \qquad b_{33}' = G_{x' \theta'} \qquad (48)$$

and

$$E_{x'} \nu_{\theta' x'} = E_{\theta'} \nu_{x' \theta'}$$

The stiffnesses of the cylinder b_{ij} are completely determined by the moduli of elasticity $E_{x'}'$, $E_{\theta'}'$, the shear modulus $G_{x'\theta'}$, the Poisson's ratio $\nu_{\theta' x'}$, and by the angle φ.

When the geometric and principal axes are parallel, i.e., $\varphi = 0$ deg,

$$b_{11} = b_{11}', \quad b_{12} = b_{12}', \quad b_{22} = b_{22}'$$

$$b_{33} = b_{33}', \quad b_{13} = b_{23} = 0 \tag{49}$$

When the geometric and principal axes are perpendicular, i.e., $\varphi = 90$ deg

$$b_{11} = b_{22}', \quad b_{12} = b_{12}', \quad b_{22} = b_{11}'$$

$$b_{33} = b_{33}', \quad b_{13} = b_{23} = 0 \tag{50}$$

When the material is isotropic,

$$b_{11} = b_{22} = \frac{E}{1-\nu^2}, \quad b_{12} = \frac{\nu E}{1-\nu^2}$$

$$b_{33} = \frac{E}{2(1+\nu)}, \quad b_{13} = b_{23} = 0 \tag{51}$$

Note that for the constant thickness orthotropic case, the stretching stiffnesses and the bending stiffnesses are not independent, i.e., from Eqs. (2) through (7) and (17) through (22), they are given by,

$$D_{ij} = \frac{1}{12} b_{ij} h^3 \qquad C_{ij} = b_{ij} h \tag{52}$$

3.2 Properties of Stiffened Cylinder

A cross section of a repeated element of the stiffened cylindrical shell is shown in Table 4. The stiffeners are aligned along the x' axis and make an angle φ with respect to the x axis.

The stretching stiffnesses, referred to the principal axes x'-y', are C'_{11}, C'_{12}, C'_{22}, C'_{33}, and may be approximated (with the assumption of no stress lag) by

$$C_{11}' = C_s\left(1+\frac{t_w}{b_y}\frac{b_w}{t_s}\right)\left[\frac{1+(1-\nu^2)\frac{t_w}{b_y}\frac{b_w}{t_s}\left(\frac{1-t_w/b_y}{1+t_s/t_w}\right)}{1+\frac{t_w}{b_y}\frac{b_w}{t_s}\left(\frac{1-t_w/b_y}{1+t_s/b_w}\right)}\right]$$

$$C_{12}' = C_{21}' = \nu C_s\left[\frac{1+\frac{t_w}{b_y}\frac{b_w}{t_s}}{1+\frac{t_w}{b_y}\frac{b_w}{t_s}\left(\frac{1-t_w/b_y}{1+t_s/t_w}\right)}\right] \qquad (53)$$

$$C_{22}' = C_s\left[\frac{1+\frac{t_w}{b_y}\frac{b_w}{t_s}}{1+\frac{t_w}{b_y}\frac{b_w}{t_s}\left(\frac{1-t_w/b_y}{1+t_s/t_w}\right)}\right]$$

$$C_{33}' = Gt_s\left[\frac{1+\frac{t_w}{b_y}\frac{b_w}{t_s}}{1+\frac{t_w}{b_y}\frac{b_w}{t_s}\left(\frac{1-t_w/b_y}{1+t_s/t_w}\right)}\right]$$

where C_s is the stretching stiffness of the basic unstiffened skin

$$C_s = \frac{Et_s}{1-\nu^2} \qquad (54)$$

The bending stiffnesses, referred to the principal axes x'-y', are D'_{11}, D'_{12}, D'_{22}, D'_{33}, and may be approximated (see Refs. 13 and 14) by

$$D_{11}' = \frac{D_s}{\left(1+\frac{b_w}{t_s}\frac{t_w}{b_y}\right)^2}\left[1+4\left(\frac{b_w}{t_s}\right)^3\frac{t_w}{b_y}(1-\nu^2)+\left(\frac{b_w}{t_s}\right)^4\left(\frac{t_w}{b_y}\right)^2\{2(1-\nu^2)+3\}\right.$$

$$\left.\left(\frac{b_w}{t_s}\right)^5\left(\frac{t_w}{b_y}\right)^3(1-\nu^2)+6\left(\frac{b_w}{t_s}\right)^2\left(\frac{t_w}{b_y}\right)\left(1-\nu^2+\frac{b_w}{t_s}\frac{t_w}{b_y}\right)+4\left(\frac{b_w}{t_s}\right)^2\left(\frac{t_w}{b_y}\right)^2\right.$$

$$\left.+\frac{b_w}{t_s}\frac{t_w}{b_y}\{3(1-\nu^2)+2\}\right]$$

$$D_{12}' = D_{21}' = \nu D_s$$

(55)

$$D_{22}' = D_s\left[\frac{1}{1-\frac{t_w}{b_y}\left\{1-\frac{1}{(1+b_w/t_s)^3}\right\}}\right]$$

$$D_{33}' = \frac{G t_s^3}{12}+\frac{C}{2b_y} = \frac{D_s(1-\nu)}{2}\left[1+6\frac{b_w}{b_y}\left(\frac{t_w}{t_s}\right)^3\beta\right]$$

where C is the torsional rigidity of the web, β is a constant based on b_w and t_w which varies from 0.333 to 0.141, and D_s is the bending stiffness of the unstiffened skin

$$D_s = \frac{1}{12}\frac{E t_s^3}{1-\nu^2} \qquad (56)$$

The thin cylindrical shell with closely-spaced stiffeners will be

considered as an equivalent orthotropic thin cylinder with given independent bending and stretching stiffnesses. With this approach and in conjunction with the stiffness transformations given by Eqs. (47), the stiffnesses C_{ij} and D_{ij} referred to the geometrical axes x-y can be written in terms of the stiffnesses C'_{ij} and D'_{ij} referred to the principal axes x'-y' as

$$(C_{11}, D_{11}) = (C_{11}', D_{11}')\cos^4\phi + (C_{22}', D_{22}')\sin^4\phi$$

$$+2\left[(C_{12}', D_{12}') + 2(C_{33}', D_{33}')\right]\cos^2\phi\sin^2\phi$$

$$(C_{12}, D_{12}) = \left[(C_{11}', D_{11}') + (C_{22}', D_{22}') - 4(C_{33}', D_{33}')\right]\cos^2\phi\sin^2\phi$$

$$+ (C_{12}', D_{12}')(\cos^4\phi + \sin^4\phi)$$

$$(C_{22}, D_{22}) = (C_{11}', D_{11}')\sin^4\phi + (C_{22}', D_{22}')\cos^4\phi$$

$$+2\left[(C_{12}', D_{12}') + 2(C_{33}', D_{33}')\right]\cos^2\phi\sin^2\phi$$

$$(C_{13}, D_{13}) = \Big[(C_{22}', D_{22}')\sin^2\phi - (C_{11}', D_{11}')\cos^2\phi - \Big\{(C_{12}', D_{12}') + 2(C_{33}', D_{33}')\Big\}(\cos^2\phi - \sin^2\phi)\Big]\cos\phi\sin\phi \tag{57}$$

$$(C_{23}, D_{23}) = \Big[(C_{22}', D_{22}')\cos^2\phi - (C_{11}', D_{11}')\sin^2\phi - \Big\{(C_{12}', D_{12}') + 2(C_{33}', D_{33}')\Big\}(\cos^2\phi - \sin^2\phi)\Big]\cos\phi\sin\phi$$

$$(C_{33}, D_{33}) = \Big[(C_{11}', D_{11}') + (C_{22}', D_{22}') - 2(C_{12}', D_{12}')\Big]\cos^2\phi\sin^2\phi + (C_{33}', D_{33}')(\cos^2\phi - \sin^2\phi)^2$$

When the geometric and principal axes are parallel, i.e., $\varphi = 0$ deg

$$\begin{aligned} &C_{11} = C_{11}', \quad C_{12} = C_{12}', \quad C_{22} = C_{22}' \\ &C_{33} = C_{33}', \quad C_{13} = C_{23} = 0 \\ &D_{11} = D_{11}', \quad D_{12} = D_{12}', \quad D_{22} = D_{22}' \\ &D_{33} = D_{33}', \quad D_{13} = D_{23} = 0 \end{aligned} \tag{58}$$

When the geometric and principal axes are perpendicular, i.e., $\varphi = 90$ deg

$$
\begin{aligned}
&C_{11} = C_{22}', \qquad C_{12} = C_{12}', \qquad C_{22} = C_{11}' \\
&C_{33} = C_{33}', \qquad C_{13} = C_{23} = 0 \\
&D_{11} = D_{22}', \qquad D_{12} = D_{12}', \qquad D_{22} = D_{11}' \\
&D_{33} = D_{33}', \qquad D_{13} = D_{23} = 0
\end{aligned}
\tag{59}
$$

3.3 Numerical Application

a) Constant Thickness Orthotropic Cylinder

Four example cylinders were selected for numerical application for the constant thickness orthotropic case and their properties are given in Table 1. Calculations for the isotropic case were also carried out for purposes of comparison. The thickness-to-radius parameter was chosen as 0.001 for these calculations. Note that for the constant thickness orthotropic case, the ratio of stretching stiffnesses and bending stiffnesses are the same, i.e.,

$$
\frac{C_{ij}}{C_{22}'} = \frac{D_{ij}}{D_{22}'} = \frac{b_{ij}}{b_{22}'} \tag{60}
$$

b) Stiffened Cylinder

Two examples of stiffened cylinders were selected whose bending stiffness ratio D_{11}'/D_{22}' is the same as those of cylinders (1) and (5) for the constant thickness orthotropic case. In order to compare the frequency spectrum for the constant thickness orthotropic cylinder and the stiffened cylinder in a meaningful

way, the term $(1/R^2)(D'_{22}/C'_{22})$ for the stiffened cylinder is set equal to $(1/12)(h/R)^2$.

4. DISCUSSION OF CALCULATIONS

4.1 Constant Thickness Orthotropic Cylinder

The general character of the frequency spectrum is indicated in Figs. 4 through 13. These curves indicate that the modes for which $n < 2$ have a different behavior than those for $n \geq 2$. The modal characteristics for $n = 0$ and $n = 1$ for the isotropic case are essentially independent of the bending stiffness of the shell (i.e., independent of h/R), since for these cases the deformation consists mainly of stretching, whereas for high n the frequency characteristics depend more strongly on bending stiffness.*

Let us consider in detail the frequency spectrum for $n = 0$. For this case one of the three roots of Eq. (42) represents the frequency of the uncoupled torsional mode, while the other two frequencies involve predominantly longitudinal and radial motion. From Eq. (39) the uncoupled torsional frequency is

$$\Omega = \pi\left(\frac{mR}{\ell}\right)\sqrt{\frac{b_{33}}{b_{22}'}\left[1+\frac{1}{3}\left(\frac{h}{R}\right)^2\right]} \tag{61}$$

while the torsional frequency of a thin-walled circular beam according to St. Venant torsion theory is

$$\Omega = \pi\left(\frac{mR}{\ell}\right)\sqrt{\frac{b_{33}}{b_{22}'}} \tag{62}$$

*For short axial wave lengths (large mR/ℓ), the effect of bending stiffness (h/R) may become important for n = 0 and 1. (See Figs. 2 and 3)

The other two frequencies also shown in Figs. 4 through 8 have as asymptotes the frequency of axial vibrations of a bar,

$$\Omega = \pi\left(\frac{mR}{\ell}\right)\sqrt{\frac{b_{11}}{b'_{22}}\left[1-\left(\frac{b_{12}}{b_{11}}\right)\left(\frac{b_{12}}{b_{22}}\right)\right]} \tag{63}$$

and the frequency of radial vibrations of a ring in plane strain for long axial wave lengths,

$$\Omega = \sqrt{\frac{b_{22}}{b'_{22}}} \tag{64}$$

and a ring in plane stress for short axial wave lengths,

$$\Omega = \sqrt{\frac{b_{22}}{b'_{22}}\left[1-\frac{b_{12}}{b_{11}}\frac{b_{12}}{b_{22}}\right]} \tag{65}$$

For the n = 0 case, the lowest frequency is not necessarily associated with predominantly radial motion. Figures 4 through 8 show that the lowest natural frequency can be associated with either the predominantly radial mode or torsional mode depending on mR/ℓ. The value of mR/ℓ for which the lowest natural frequency changes from the predominantly radial mode to the torsional mode depends on the stiffness ratio b'_{11}/b'_{22} and the angle φ. From Figs. 4 through 8, it is observed that the torsional frequency is slightly affected by the stiffness ratios b'_{11}/b'_{22} and the angle φ, while the axial frequency, since it depends mainly on the stiffness in the axial direction, is affected by the stiffness ratio b'_{11}/b'_{22} only when $\varphi = 0$ deg. It also may be noted that the rise in the predominantly radial frequency at very short axial wave lengths (large mR/ℓ) is due to the effect of h/R.

Let us turn now to the case for n = 1. Here, for long axial wave lengths (small mR/ℓ), the mode associated with the lowest frequency involves strong coupling in the circumferential and radial directions. For long axial wave lengths, this corresponds to the vibration of a cylinder as a beam. The asymptotes for cases (1) and (5) that are shown in Fig.14 are those of a simply-supported thin-walled circular cross-sectioned beam as found from elementary beam theory to be

$$\Omega = \pi^2 \left(\frac{mR}{\ell}\right)^2 \sqrt{\frac{1}{2}\frac{b_{11}}{b'_{22}}\left[1-\left(\frac{b_{12}}{b_{11}}\right)\left(\frac{b_{12}}{b_{22}}\right)\right]} \qquad (66)$$

Figures 9 through 13 show that for long axial wave lengths (small mR/ℓ) circumferential stiffening has a negligible effect on the beam-type frequencies while axial stiffening has a significant effect; whereas for short axial wave lengths (large mR/ℓ) axial stiffening has a slight effect and circumferential stiffening has a significant effect on the frequency.

Now let us consider the case for $n \geq 2$. The asymptotic values of the three frequencies for long axial wave lengths (small mR/ℓ) are (for $\bar{n}_x = \bar{n}_\theta = 0$):

Flexural vibrations of a ring ($\epsilon_{\theta_o} = 0$, $u = 0$)

$$\Omega = \frac{1}{2}\left(\frac{h}{R}\right)\sqrt{\frac{1}{3}\frac{b_{22}}{b'_{22}}\left[1-\left(\frac{b_{12}}{b_{11}}\right)\left(\frac{b_{12}}{b_{22}}\right)\right]\frac{n^2(n^2-1)^2}{n^2+1}} \qquad (67)$$

Axial shear vibration (w = v = 0)

$$\Omega = \sqrt{\frac{b_{33}}{b'_{22}}}\,\kappa \tag{68}$$

Extensional vibrations of a ring (κ_θ = 0, u = 0)

$$\Omega = \sqrt{\frac{b_{22}}{b'_{22}}\left[1-\left(\frac{b_{12}}{b_{11}}\right)\left(\frac{b_{12}}{b_{22}}\right)\right](n^2+1)} \tag{69}$$

For the $n \geq 2$ cases, the lowest frequency corresponds to the predominantly radial mode for all values of mR/ℓ and stiffnesses, while the remaining two correspond to predominantly axial and circumferential motion. In general, these two are at least an order of magnitude higher than the predominantly radial frequency. From Figs. 9 through 13, the effect of the stiffness ratio and the rotation of the principal axes of stiffness through an angle of 90 degrees can be studied. It may be seen that stiffness ratio b'_{11}/b'_{22} has little effect on the predominantly radial frequency for long and intermediate axial wave lengths when φ = 0 deg (axial stiffening), while this frequency shows a marked increase when the stiffness ratio b'_{11}/b'_{22} increases for φ = 90 deg (circumferential stiffening). Specifically, it may be noted that for mR/ℓ = 0.01, n = 3, b'_{11}/b'_{22} = 24.2, when φ = 0 deg the frequency is 0.00225, and when φ = 90 deg, the frequency is 0.0108; while for the corresponding isotropic case, the frequency is 0.00219. For all values of stiffening both in circumferential, as well as axial direction for large axial wave lengths, the frequency is proportional to n^2 (for sufficiently high n) as indicated by Eq. (67).

In all the cases of stiffening for $n \geq 2$, the value of n for which the minimum frequency occurs, increases with increasing mR/ℓ. This is also true for the isotropic case.

4.2 Stiffened Cylinder

In the preceding section, the results were obtained from the analysis of a cylindrical shell which was orthotropic due to the natural properties of the material. Here we will consider a shell which is orthotropic due to attachment of stiffeners on to the basic thin-walled cylinder. The purpose of this analysis will be to compare the frequency characteristics obtained from a study of the stiffened cylinder with those obtained from the constant thickness orthotropic cylinder.

Figures 15 through 18 show the results of the stiffened cylinder analysis. The properties of the cylinders are given in Table 4. The essential difference in the properties of the stiffened cylinder and the constant thickness orthotropic cylinder is that in the former, the stretching stiffness and bending stiffness ratio are quite different while in the latter case they are identical. In particular, for the stiffened cylinders considered in this section, when the bending stiffness ratio D'_{11}/D'_{22} was taken to be the same as that of the bending stiffness ratio in Cases 1 and 5 of the constant thickness orthotropic cylinder, namely $D'_{11}/D'_{22} = 24.2$, the stretching stiffness ratio C'_{11}/C'_{22} in the case of the stiffened shell was 1.26. Returning to Figs. 15 through 18 one finds that for the $n = 0$ and $n = 1$ cases, which correspond to predominantly stretching of the shell middle surface, the values of the frequency are approximately the same as those of the isotropic case.*

*For $\varphi = 0$ deg and $n = 0$, there is a slight increase in the frequency (when compared with the isotropic case) of the mode associated with predominantly axial motion since this frequency is effectively proportional to $\sqrt{C'_{11}/C'_{22}}$. This increase is also true for the $n = 1$ case when $\varphi = 0$ and $mR/\ell > 5$, due to the slight effect of bending for these high values of mR/ℓ.

For the $n \geq 2$ cases, the effect of bending becomes extremely important even for n as low as 2. If we compare Fig. 17 with Fig. 9 (which correspond to $\varphi = 90$ deg), it is evident that the values of the predominantly radial frequency for the stiffened cylinder are approximately the same as those of the constant thickness orthotropic cylinder when $mR/\ell < 0.5$, and $n \geq 2$. For higher values of mR/ℓ, the frequency of the stiffened cylinder decreases below that of the corresponding constant thickness orthotropic cylinder for all values of $n \geq 2$. Note that this decrease diminishes with increasing n, so that for very high n, the frequencies for both these cylinders (constant thickness and stiffened) again become approximately the same. This is explained by the fact that for large values of n and mR/ℓ the influence of bending is predominant. When the stiffeners are aligned in the axial direction ($\varphi = 0$ deg), one observes from Figs. 13 and 18 that for $n \geq 4$, frequencies for both type cylinders are nearly the same for long axial wave lengths (low mR/ℓ); for intermediate axial wave lengths, the difference in the frequency for these cylinders becomes appreciable, while for short axial wave lengths, this difference again becomes small. For n = 2 and 3, the frequency of the cylinder with axial stiffeners is lower than the corresponding constant thickness orthotropic cylinder for all but short axial wave lengths.

4.3 Effect of Internal Pressure

For a closed-end cylinder under internal pressure p,

$$\bar{n}_\theta = \frac{pR}{C_{22}'} \quad , \qquad \bar{n}_x = \frac{\bar{n}_\theta}{2} \tag{70}$$

In order to gain some physical insight into the magnitude of the pressure stiffness parameter $\bar{n}_\theta$, one can express $\bar{n}_\theta$ in terms of the initial static circumferential stress $\bar{\sigma}_\theta$ as follows,

$$\bar{\sigma}_\phi = \left(\frac{C'_{22}}{h_{min}}\right)\bar{n}_\theta \tag{71}$$

For the constant thickness orthotropic cylinder

$$\bar{\sigma}_\theta = \frac{E_{\theta'}}{1-\nu_{\theta'x'}\nu_{x'\theta'}}\bar{n}_\theta$$

With $\nu_{\theta'x'} = \nu_{x'\theta'} = 0.3$, $E_{\theta'} = 10^7$ psi. This becomes

$$\bar{\sigma}_\theta = 1.1 \times 10^7 \bar{n}_\theta \text{ psi.}$$

Shown in Figs. 19 through 21 is the variation of Ω_1 with the pressure stiffness parameters $\bar{n}_\theta$, $\bar{n}_x$ for the isotropic case* for three values of the axial wave length. Comparison of these figures shows that the value of n for which the lowest frequency begins to vary significantly with $\bar{n}_\theta$ depends on the axial wave length mR/ℓ. For $mR/\ell = 0.06$ there is a significant increase in Ω_1 with $\bar{n}_\theta$ when $n \geq 2$, for $mR/\ell = 0.5$ the increase becomes significant when $n \geq 5$, and for $mR/\ell = 3$ when $n \geq 10$. For all these values of mR/ℓ, the two larger frequencies, which correspond to predominantly tangential motions, are little affected by $\bar{n}_\theta$, $\bar{n}_x$.

a) Constant Thickness Orthotropic Cylinder

The effect of internal pressure on the frequencies of the axisymmetric mode ($n = 0$) is illustrated in Figs. 4 through 8. For both $\varphi = 0$ and 90 degrees and all values of stiffening, the frequency of the predominantly radial mode is slightly increased by the addition of internal pressure at high values of mR/ℓ. The increase in the frequency of the torsional mode, due to pressure,

*In all the pressure investigations, $\bar{n}_x$ is always included, and is taken equal to $\bar{n}_\theta/2$.

increases with increasing b'_{11}/b'_{22} and is the same for $\varphi = 0$ and 90 degrees. This increase in frequency diminishes rapidly with increasing values of mR/ℓ. Internal pressure has a negligible effect on the predominantly axial frequency when $\varphi = 0$ and 90 degrees for all values of the stiffness ratio b'_{11}/b'_{22}.

For the $n = 1$ mode, the effect of pressure on the lowest frequency is shown in Figs. 22 through 26. For stiffening in the circumferential direction ($\varphi = 90$ deg) the frequency is independent of the stiffness ratio b'_{11}/b'_{22}. There is an increase in frequency due to pressure in these cases, which is large for small values of mR/ℓ and diminishes with increasing mR/ℓ. For stiffening in the axial direction ($\varphi = 0$ deg), the frequency does depend on the stiffness ratio b'_{11}/b'_{22}. There is an increase in frequency in these cases, which is small for low values of mR/ℓ, diminishes for intermediate values of mR/ℓ, and increases for high values of mR/ℓ. The effect of pressure on the two higher frequencies for $n = 1$ is negligible.

For $n \geq 2$, Figs. 22 through 26 show that the lowest frequency increases significantly with internal pressure for all cases of stiffening. The increase in the frequency generally diminishes with increasing mR/ℓ. It is observed that the increase in frequency due to pressure is greater for stiffening in the axial direction than in the circumferential direction. Thus for $mR/\ell = 0.01$, $b'_{11}/b'_{22} = 24.2$, and $n = 2$, for stiffening in the circumferential direction ($\varphi = 90$ deg), the unpressurized frequency $\Omega_1 = 0.00383$, while in the corresponding case of axial stiffening ($\varphi = 0$ deg), $\Omega_1 = 0.00130$. However, with the addition of internal pressure ($\bar{n}_\theta = 2\bar{n}_x = 0.001$), when $\varphi = 90$ deg the frequency $\Omega_1 = 0.0426$, while for $\varphi = 0$ deg, $\Omega_1 = 0.0424$. This same pattern of behavior, namely the influence of internal pressure on the frequency being greater for axial stiffening than for circumferential stiffening, is found for all $n > 2$ as well as $n = 2$. Also illustrated in Figs. 22 through 26 is the fact that for

φ = 90 deg, the increase in frequency due to internal pressure decreases with increasing values of the stiffness ratio b'_{11}/b'_{22}, while for φ = 0 deg, this increase is independent of b'_{11}/b'_{22}. For $n \geq 2$, internal pressure has a negligible effect on the two larger frequencies.

b) Stiffened Cylinder

The effect of pressure on the n = 0 mode for the stiffened cylinder is similar to that of the isotropic case. This is due to the fact that the stretching stiffness ratio C'_{11}/C'_{22} of the stiffened cylinder and the isotropic cylinder are nearly the same. For both φ = 0 and 90 degrees, the frequency of the predominantly radial mode is slightly increased by internal pressure for high mR/ℓ. The increase in the frequency of the torsional mode due to internal pressure is the same for φ = 0 and 90 degrees and again diminishes rapidly with increasing mR/ℓ. The axial frequency is unaffected by internal pressure for both φ = 0 and 90 degrees.

Turning to the n = 1 case, Figs. 17 and 18 show that the increase in frequency due to pressure is approximately the same as that of the isotropic case for φ = 0 and 90 degrees (except for $mR/\ell > 5$ where the bending stiffness ratio D'_{11}/D'_{22} begins to take effect).

For $n \geq 2$, the frequencies of the stiffened cylinders under internal pressure are the same as those of the constant thickness orthotropic shell (i.e., cylinders 1 and 5), except for large values of mR/ℓ. The effect of pressure on the two higher frequencies for $n \geq 1$ is negligible.

5. CONCLUSIONS

The equations for the vibration of a thin orthotropic cylindrical shell under internal pressure were deduced from the nonlinear shell theory of Washizu. Application was made to four constant thickness orthotropic cylinders, two stiffened cylinders, and for purposes of comparison, an isotropic cylinder. This investigation has been principally concerned with the effects of circumferential and axial stiffening, as well as internal pressure, on the frequencies and mode shapes of an orthotropic cylinder with freely-supported ends.

The significant conclusions are that there is a difference in behavior of the frequencies for the $n = 0$, $n = 1$, and $n \geq 2$ modes. For the $n \geq 2$ modes, the lowest frequency is associated with predominantly radial motion. For the $n = 0$ mode, the lowest frequency is associated with either the uncoupled torsional motion or the predominately radial motion, depending on the axial wave length. For the $n = 1$ mode, there is strong coupling between circumferential and radial motion, and the lowest frequency is associated with a combination of circumferential and radial motion.

For the $n \geq 2$ modes, the frequency of the predominantly radial frequency was significantly increased by circumferential stiffening, while this frequency was unaffected by axial stiffening for all but large values of mR/ℓ. For the $n = 0$ mode, there was a slight increase in the frequencies of the torsional mode and predominantly radial modes due to circumferential stiffening, while the frequency of the predominantly axial mode was unchanged. For axial stiffening, the frequency of the predominantly axial mode was significantly increased, while the frequency of the torsional and predominantly radial modes was slightly affected. For

the n = 1 mode, circumferential stiffening increased the frequency only for large values of mR/ℓ, while axial stiffening increased the frequency mainly for small mR/ℓ.

The effect of pressure on the frequencies was also investigated. For the $n \geq 2$ modes, for both circumferential and axial stiffening, the predominantly radial frequencies were significantly increased by pressure. For the n = 0 mode, for both circumferential and axial stiffening, the torsional frequency was increased by pressure at small mR/ℓ and the predominantly radial frequency was increased by pressure at large mR/ℓ. The predominantly axial frequency was not affected by pressure. For the n = 1 mode, for circumferential stiffening, the frequency was increased by pressure at small mR/ℓ, while for axial stiffening the frequency was slightly increased by pressure.

For purposes of comparison, the frequencies of two stiffened cylinders were also investigated. It was found that the frequencies of the stiffened cylinders whose bending stiffness ratio D'_{11}/D'_{22} was taken equal to the stiffness ratio b'_{11}/b'_{22} of the constant thickness orthotropic cylinder are essentially the same as the frequencies of the isotropic cylinder for n = 0 and n = 1 modes, while for the $n \geq 2$ modes the stiffened cylinder frequencies are the same as the frequencies of the constant thickness orthotropic cylinder. This occurs since the n = 0 and 1 modes correspond to primarily stretching motion, while the $n \geq 2$ modes correspond to predominantly bending motion. The above behavior is true for both the pressurized as well as the unpressurized cases.

REFERENCES

1. Arnold, R. N., and Warburton, G. B. Flexural Vibrations of the Walls of Thin Cylindrical Shells Having Freely Supported Ends. Proceedings of the Royal Society, (London), Series A, Vol. 197, 1949.

2. Goldenveizer, A. L. Theory of Thin Elastic Shells. (English Translation) Pergamon Press.

3. Reissner, E. Non-Linear Effects in Vibrations of Cylindrical Shells. Aeromechanics Report No. AM 5-6, Ramo-Wooldridge Corp., August 1955.

4. Reissner, E. Notes on Vibrations of Thin, Pressurized Cylindrical Shells. Aeromechanics Report AM 5-4, Ramo-Wooldridge Corp., November 1955.

5. Fung, Y. C., Sechler, E. E., and Kaplan, A. On the Vibration of Thin Cylindrical Shells under Internal Pressure. Journal of the Aeronautical Sciences, Vol. 24, No. 9, September 1957.

6. Timoshenko, S. P., and Gere, J. M. Theory of Elastic Stability. McGraw-Hill Book Co., Inc., New York, 1961.

7. Armenákas, A. E. On the Influence of Initial Stress on the Vibrations of Simply Supported Circular Cylindrical Shells. PIBAL Report, No. 673, October 1963.

8. Herrmann, G., and Armenákas, A. E. Dynamic Behavior of Cylindrical Shells under Initial Stress. Proceedings Fourth U. S. National Congress of Applied Mechanics, ASME, 1962.

9. Forsberg, K. Influence of Boundary Conditions of the Modal Characteristics of Thin Cylindrical Shells. American Institute of Aeronautics and Astronautics Journal, Vol. 2, No. 12, December, 1964.

10. Washizu, K. Some Considerations on Shell Theory. Massachusetts Institute of Technology, Aeroelastic and Structures Research Laboratory, Technical Report No. 1001, October 1960.

11. Bisplinghoff, R. L., and Ashley, H. Principles of Aeroelasticity. John Wiley and Sons, Inc., 1962.

12. Hearmon, R. F. S. An Introduction to Applied Anisotropic Elasticity. Oxford University Press, 1961.

13. Dow, N. F., Libone, C., and Hubka, R. E. Formulas for the Elastic Constants of Plates with Integral Waffle-Like Stiffening. NACA TR 1195, 1954.

14. Timoshenko, S., and Woinowsky-Krieger, S. Theory of Plates and Shells. Second Edition, McGraw-Hill Book Co., Inc., 1949.

15. Donnell, L. H. Stability of Thin-Walled Tubes under Torsion. NACA Report 479, 1933.

16. Novozhilov, V. V. The Theory of Thin Shells. P. Noordhoff LTD., Groningen, The Netherlands, 1959.

17. Flügge, W. Stress in Shells. Springer-Verlag, Berlin, 1962.

18. Budiansky, B., and Sanders, J. L. On the "Best" First-Order Linear Shell Theory. Harvard University, Division of Engineering and Applied Physics, Technical Report No. 14, September 1962.

19. Koiter, W. T. A Consistent First Approximation in the General Theory of Thin Elastic Shells. Proceedings of the Symposium in the Theory of Thin Elastic Shells, Delft, 1959, Edited by W. T. Koiter, North-Holland Publishing Co., Amsterdam 1960.

TABLE 1
$(1/R^2)(D'_{22}/C'_{22})$ Terms for Various Thin Cylindrical Shell Theories

	$F_1(u,v,w)$	$F_2(u,v,w)$	$F_3(u,v,w)$
Donnell (Ref.15)	0	0	0
Timoshenko (Ref.6)	0	$2\frac{D_{33}}{D'_{22}}\frac{\partial^2 v}{\partial x^2} + \frac{3}{R}\frac{D_{23}}{D'_{22}}\frac{\partial^2 v}{\partial x \partial \theta} + \frac{1}{R^2}\frac{D_{22}}{D'_{22}}\frac{\partial^2 v}{\partial \theta^2} + R\frac{D_{13}}{D'_{22}}\frac{\partial^3 w}{\partial x^3} + \frac{D_{12}+2D_{33}}{D'_{22}}\frac{\partial^3 w}{\partial x^2 \partial \theta} + \frac{3}{R}\frac{D_{23}}{D'_{22}}\frac{\partial^3 w}{\partial x \partial \theta^2} + \frac{1}{R^2}\frac{D_{22}}{D'_{22}}\frac{\partial^3 w}{\partial \theta^3}$	$-\left[2R\frac{D_{13}}{D'_{22}}\frac{\partial^3 v}{\partial x^3} + \frac{D_{12}+4D_{33}}{D'_{22}}\frac{\partial^3 v}{\partial x^2 \partial \theta} + \frac{4}{R}\frac{D_{23}}{D'_{22}}\frac{\partial^3 v}{\partial x \partial \theta^2} + \frac{1}{R^2}\frac{D_{22}}{D'_{22}}\frac{\partial^3 v}{\partial \theta^3} + 4R\frac{D_{13}}{D'_{22}}\frac{\partial^4 w}{\partial x^3 \partial \theta} + \frac{4}{R}\frac{D_{23}}{D'_{22}}\frac{\partial^4 w}{\partial x \partial \theta^3}\right]$
Washizu (Ref.10) Novozhilov (Ref.16) and Goldenveizer (Ref.2)	0	$4\frac{D_{33}}{D'_{22}}\frac{\partial^2 v}{\partial x^2} + \frac{4}{R}\frac{D_{23}}{D'_{22}}\frac{\partial^2 v}{\partial x \partial \theta} + \frac{1}{R^2}\frac{D_{22}}{D'_{22}}\frac{\partial^2 v}{\partial \theta^2} + 2R\frac{D_{13}}{D'_{22}}\frac{\partial^3 w}{\partial x^3} + \frac{D_{12}+4D_{33}}{D'_{22}}\frac{\partial^3 w}{\partial x^2 \partial \theta} + \frac{4}{R}\frac{D_{23}}{D'_{22}}\frac{\partial^3 w}{\partial x \partial \theta^2} + \frac{1}{R^2}\frac{D_{22}}{D'_{22}}\frac{\partial^3 w}{\partial \theta^3}$	$-\left[2R\frac{D_{13}}{D'_{22}}\frac{\partial^3 v}{\partial x^3} + \frac{D_{12}+4D_{33}}{D'_{22}}\frac{\partial^3 v}{\partial x^2 \partial \theta} + \frac{4}{R}\frac{D_{23}}{D'_{22}}\frac{\partial^3 v}{\partial x \partial \theta^2} + \frac{1}{R^2}\frac{D_{22}}{D'_{22}}\frac{\partial^3 v}{\partial \theta^3} + 4R\frac{D_{13}}{D'_{22}}\frac{\partial^4 w}{\partial x^3 \partial \theta} + \frac{4}{R}\frac{D_{23}}{D'_{22}}\frac{\partial^4 w}{\partial x \partial \theta^3}\right]$

TABLE 1 (Continued)

	$F_1(u,v,w)$	$F_2(u,v,w)$	$F_3(u,v,w)$
Flügge (Ref.17) and Herrmann, Armenakas (Ref.8)	$\frac{1}{R^2}\frac{D_{33}}{D'_{22}}\frac{\partial^2 u}{\partial\theta^2}+\frac{D_{13}}{D'_{21}}\frac{\partial^2 v}{\partial x^2}$ $+R\frac{D_{11}}{D'_{22}}\frac{\partial^3 w}{\partial x^3}+\frac{D_{13}}{D'_{22}}\frac{\partial^3 w}{\partial x^2\partial\theta}$ $-\frac{1}{R}\frac{D_{33}}{D'_{22}}\frac{\partial^3 w}{\partial x\partial\theta^2}-\frac{1}{R}\frac{D_{23}}{D'_{21}}\frac{\partial^3 w}{\partial\theta^3}$ $-\frac{1}{R^2}\frac{D_{23}}{D'_{21}}\frac{\partial w}{\partial\theta}$	$\frac{D_{13}}{D'_{21}}\frac{\partial^2 u}{\partial x^2}+3\frac{D_{33}}{D'_{21}}\frac{\partial^2 v}{\partial x^2}+\frac{2}{R}\frac{D_{23}}{D'_{21}}\frac{\partial^2 v}{\partial x\partial\theta}$ $+2R\frac{D_{13}}{D'_{22}}\frac{\partial^3 w}{\partial x^3}+\frac{D_{12}+3D_{33}}{D'_{22}}\frac{\partial^3 w}{\partial x^2\partial\theta}$ $+\frac{2}{R}\frac{D_{23}}{D'_{22}}\frac{\partial^3 w}{\partial x\partial\theta^2}$	$-\left[R\frac{D_{11}}{D'_{22}}\frac{\partial^2 u}{\partial x^2}+\frac{D_{13}}{D'_{21}}\frac{\partial^2 u}{\partial x\partial\theta}-\frac{1}{R}\frac{D_{23}}{D'_{21}}\frac{\partial^2 u}{\partial x\partial\theta^2}\right.$ $-\frac{1}{R^2}\frac{D_{23}}{D'_{22}}\frac{\partial u}{\partial\theta}+2R\frac{D_{13}}{D'_{22}}\frac{\partial^2 v}{\partial x^2}$ $+\frac{D_{12}+3D_{33}}{D'_{22}}\frac{\partial^2 v}{\partial x\partial\theta}+\frac{2}{R}\frac{D_{23}}{D'_{21}}\frac{\partial^2 v}{\partial x\partial\theta^2}$ $+\frac{4}{R}\frac{D_{23}}{D'_{22}}\frac{\partial^2 w}{\partial x\partial\theta^2}+4R\frac{D_{13}}{D'_{21}}\frac{\partial^2 w}{\partial x^2\partial\theta}$ $\left.+\frac{2}{R}\frac{D_{23}}{D'_{22}}\frac{\partial^2 w}{\partial x\partial\theta}+\frac{2}{R}\frac{D_{12}}{D'_{22}}\frac{\partial^2 w}{\partial\theta^2}+\frac{D_{12}}{D'_{21}}\frac{w}{R^2}\right]$
Budiansky, Sanders (Ref.18) and Koiter (Ref.19)	$\frac{1}{4R^2}\frac{D_{33}}{D'_{22}}\frac{\partial^2 u}{\partial\theta^2}-\frac{3}{4R}\frac{D_{33}}{D'_{22}}\frac{\partial^2 v}{\partial x\partial\theta}$ $-\frac{1}{2R^2}\frac{D_{23}}{D'_{22}}\frac{\partial^2 v}{\partial\theta^2}-\frac{1}{2}\frac{D_{13}}{D'_{21}}\frac{\partial^3 w}{\partial x^2\partial\theta}$ $-\frac{1}{R}\frac{D_{33}}{D'_{21}}\frac{\partial^3 w}{\partial x\partial\theta^2}-\frac{1}{2R^2}\frac{D_{12}}{D'_{22}}\frac{\partial^3 w}{\partial\theta^3}$	$-\frac{3}{4R}\frac{D_{33}}{D'_{22}}\frac{\partial^2 u}{\partial x\partial\theta}-\frac{1}{2R^2}\frac{D_{23}}{D'_{21}}\frac{\partial^2 u}{\partial\theta^2}+\frac{9}{4}\frac{D_{33}}{D'_{21}}\frac{\partial^2 v}{\partial x^2}$ $+\frac{3}{R}\frac{D_{23}}{D'_{22}}\frac{\partial^2 v}{\partial x\partial\theta}+\frac{1}{R^2}\frac{D_{12}}{D'_{21}}\frac{\partial^2 v}{\partial\theta^2}+\frac{3}{2}R\frac{D_{13}}{D'_{21}}\frac{\partial^3 w}{\partial x^3}$ $+\frac{D_{12}+3D_{33}}{D'_{22}}\frac{\partial^3 w}{\partial x^2\partial\theta}+\frac{7}{2R}\frac{D_{23}}{D'_{22}}\frac{\partial^3 w}{\partial x\partial\theta^2}$ $+\frac{1}{R^2}\frac{D_{22}}{D'_{22}}\frac{\partial^3 w}{\partial\theta^3}$	$\frac{1}{2}\frac{D_{13}}{D'_{22}}\frac{\partial^3 u}{\partial x^2\partial\theta}+\frac{1}{R}\frac{D_{33}}{D'_{21}}\frac{\partial^3 u}{\partial x\partial\theta^2}+\frac{1}{2R^2}\frac{D_{23}}{D'_{21}}\frac{\partial^3 u}{\partial\theta^3}$ $-\frac{3}{2}R\frac{D_{13}}{D'_{21}}\frac{\partial^3 v}{\partial x^3}-\frac{D_{12}+3D_{33}}{D'_{21}}\frac{\partial^3 v}{\partial x^2\partial\theta}$ $-\frac{7}{2R}\frac{D_{23}}{D'_{22}}\frac{\partial^3 v}{\partial x\partial\theta^2}-\frac{1}{R^2}\frac{D_{22}}{D'_{21}}\frac{\partial^3 v}{\partial\theta^3}$ $-4R\frac{D_{13}}{D'_{21}}\frac{\partial^4 w}{\partial x^3\partial\theta}-\frac{4}{R}\frac{D_{23}}{D'_{22}}\frac{\partial^4 w}{\partial x\partial\theta^3}$

TABLE 2
Initial Stressing Functions for Various Thin Cylindrical Shell Theories

	$G_1(\bar{N}_x, \bar{N}_\theta, u, v, w)$	$G_2(\bar{N}_x, \bar{N}_\theta, u, v, w)$	$G_3(\bar{N}_x, \bar{N}_\theta, u, v, w)$
Timoshenko (Ref.6)	$-\frac{\bar{n}_\theta}{R}\left(\frac{\partial^2 v}{\partial x \partial \theta} - \frac{\partial w}{\partial x}\right)$	$\bar{n}_x \frac{\partial^2 v}{\partial x^2}$	$\bar{n}_x \frac{\partial^2 w}{\partial x^2} + \frac{\bar{n}_\theta}{R^2}\left(\frac{\partial v}{\partial \theta} + \frac{\partial^2 w}{\partial \theta^2}\right)$
Washizu (Ref.10) and Herrmann, Armenákas (Ref.8)	$\bar{n}_x \frac{\partial^2 u}{\partial x^2} + \frac{\bar{n}_\theta}{R^2}\frac{\partial^2 u}{\partial \theta^2}$	$\bar{n}_x \frac{\partial^2 v}{\partial x^2} + \frac{\bar{n}_\theta}{R^2}\left(\frac{\partial^2 v}{\partial \theta^2} - 2\frac{\partial w}{\partial \theta} - v\right)$	$\bar{n}_x \frac{\partial^2 w}{\partial x^2} + \frac{\bar{n}_\theta}{R^2}\left(2\frac{\partial v}{\partial \theta} + \frac{\partial^2 w}{\partial \theta^2} - w\right)$
Flügge (Ref.17)	$\bar{n}_x \frac{\partial^2 u}{\partial x^2} + \frac{\bar{n}_\theta}{R^2}\left(\frac{\partial^2 u}{\partial \theta^2} + R\frac{\partial w}{\partial x}\right)$	$\bar{n}_x \frac{\partial^2 v}{\partial x^2} + \frac{\bar{n}_\theta}{R^2}\left(\frac{\partial^2 v}{\partial \theta^2} - \frac{\partial w}{\partial \theta}\right)$	$\bar{n}_x \frac{\partial^2 w}{\partial x^2} + \frac{\bar{n}_\theta}{R^2}\left(-\frac{\partial u}{\partial x} + \frac{\partial v}{\partial \theta} + \frac{\partial^2 w}{\partial \theta^2}\right)$

TABLE 3

Properties of Example Constant Thickness Orthotropic Cylinders

CYLINDER	φ	$\frac{b'_{11}}{b'_{22}}$	$\frac{b'_{12}}{b'_{22}}$	$\frac{b'_{33}}{b'_{22}}$	$\frac{h}{R}$
1	90^{o}	24.2	.270	.527	.001
2	90^{o}	5.35	.273	.405	.001
3 (Isotropic)	--	1	.3	.35	.001
4	0^{o}	5.35	.273	.405	.001
5	0^{o}	24.2	.270	.527	.001

TABLE 4
Properties of Example Stiffened Cylinders

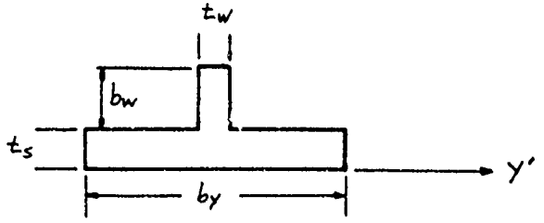

CYLINDER	φ	$\frac{b_w}{t_s}$	$\frac{t_w}{b_y}$	$\frac{t_w}{t_s}$	β	$\frac{C'_{11}}{C'_{22}}$	$\frac{C'_{12}}{C'_{22}}$	$\frac{C'_{33}}{C'_{22}}$	$\frac{D'_{11}}{D'_{22}}$	$\frac{D'_{12}}{D'_{22}}$	$\frac{D'_{33}}{D'_{22}}$	$\frac{1}{R^2}\frac{D'_{22}}{C'_{22}}$
6	90^o	4	.10	.40	.280	1.26	.3	.35	24.2	.270	.527	$\frac{1}{12}(.001)^2$
7	0^o	4	.10	.40	.280	1.26	.3	.35	24.2	.270	.527	$\frac{1}{12}(.001)^2$

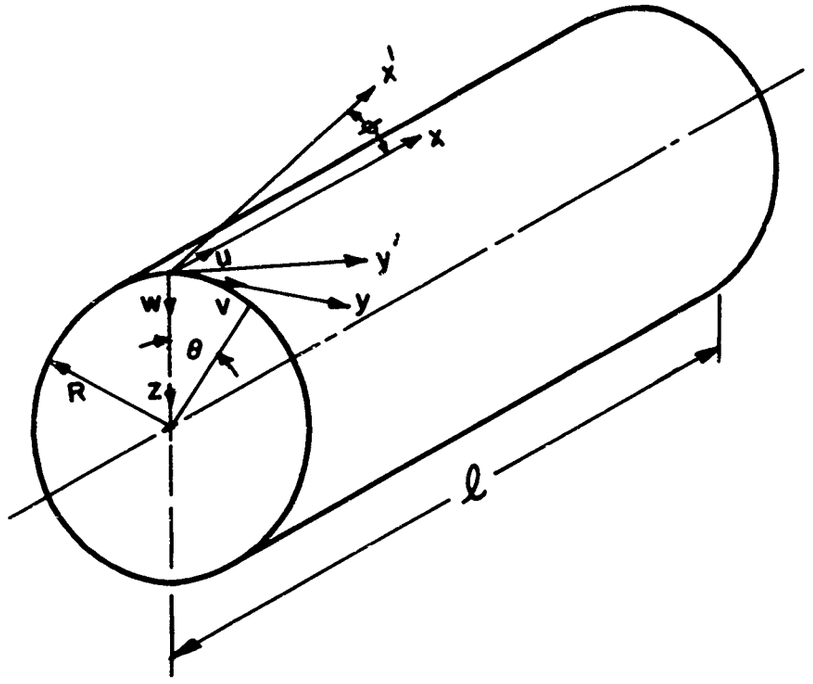

1a

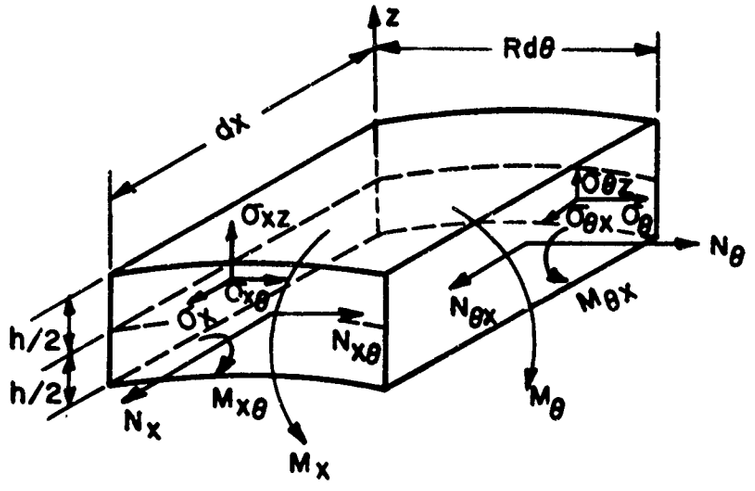

1b

FIG. 1 SHELL MIDDLE SURFACE AND SHELL ELEMENT

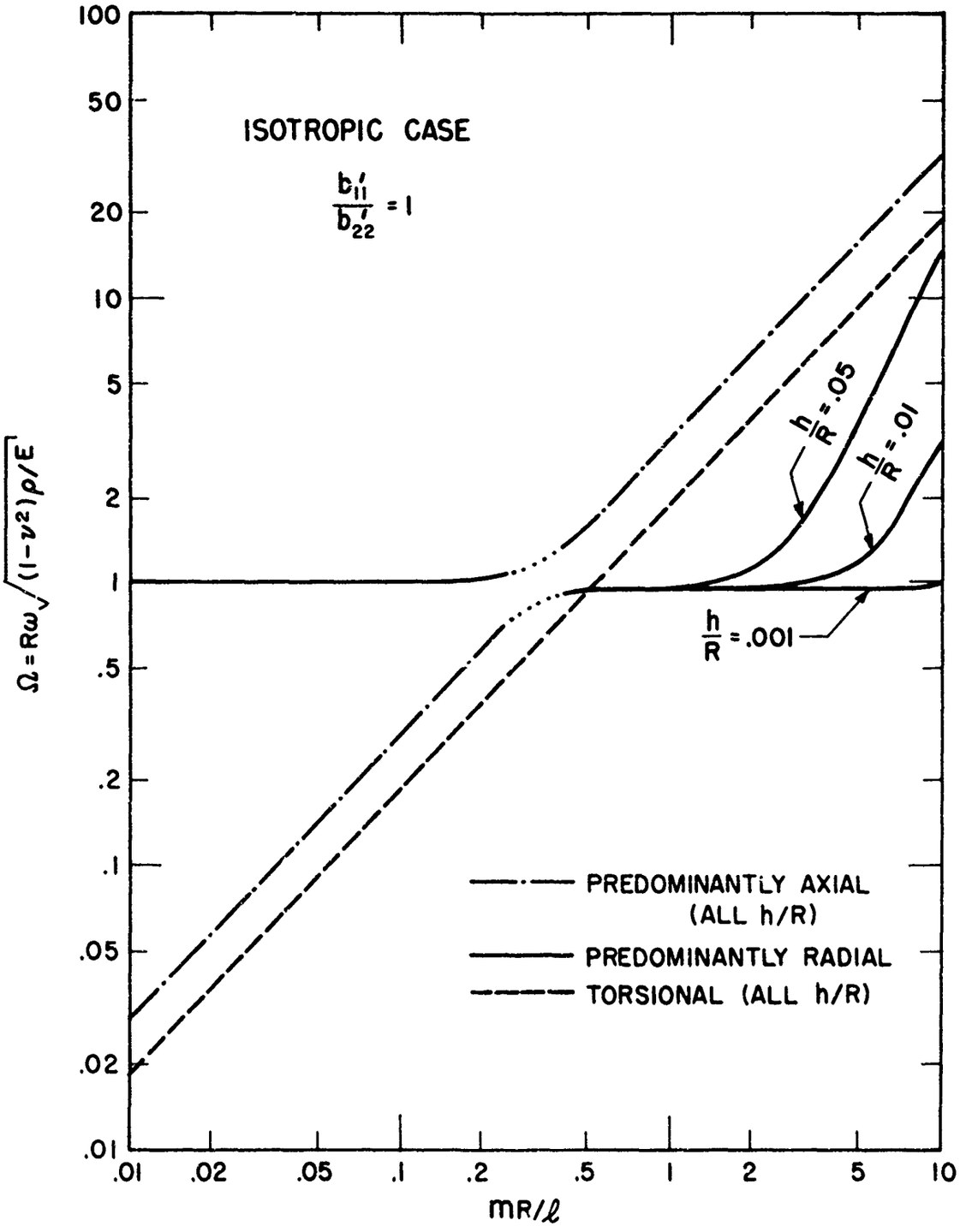

FIG. 2 EFFECT OF h/R ON FREQUENCY DISTRIBUTION OF n = 0 MODE FOR ISOTROPIC CYLINDER

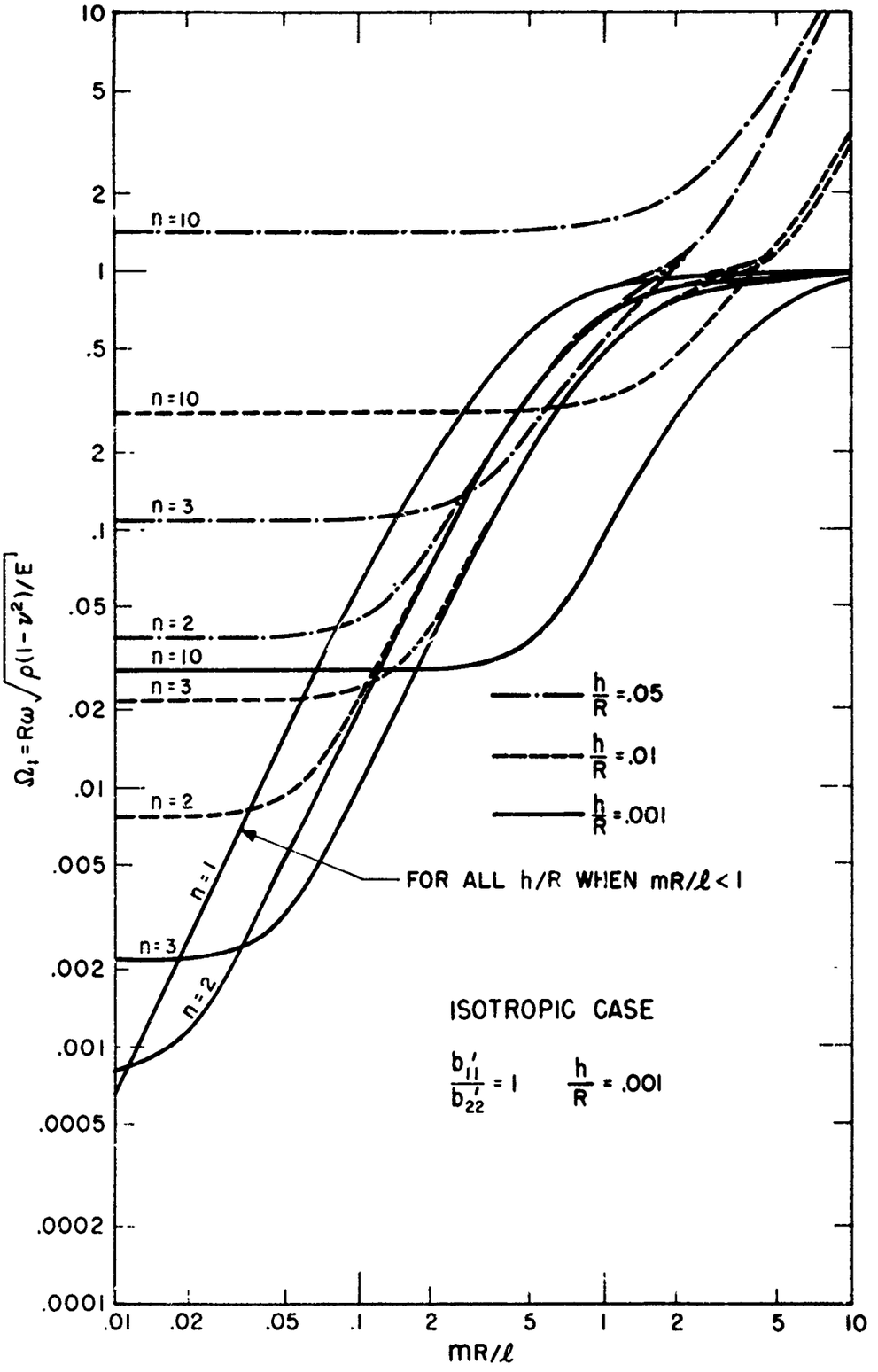

FIG. 3 EFFECT OF h/R ON FREQUENCIES OF n≥1 MODES FOR ISOTROPIC CYLINDER

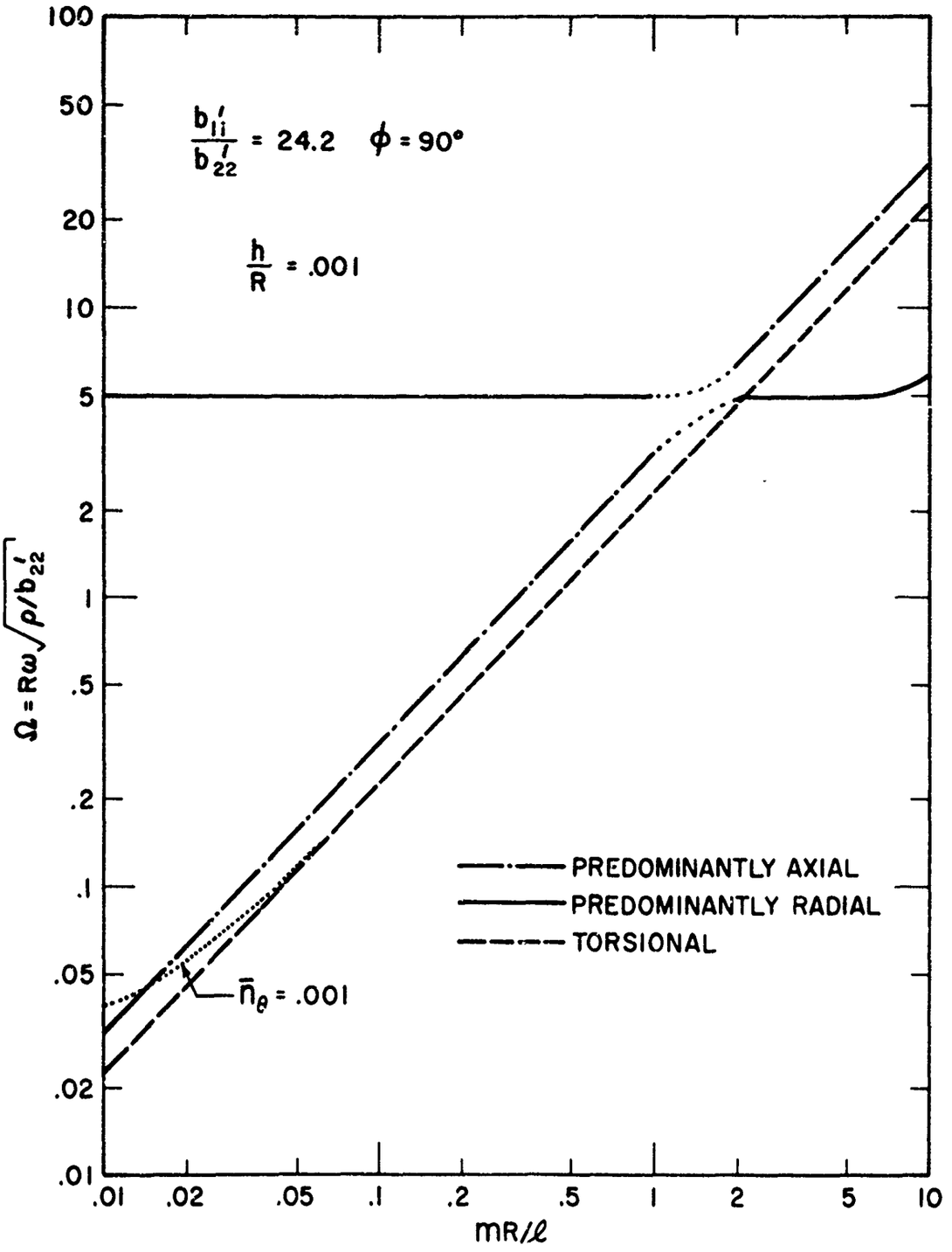

FIG. 4 FREQUENCY DISTRIBUTION OF n=0 MODE FOR CIRCUMFERENTIAL STIFFENING — CONSTANT THICKNESS ORTHOTROPIC CYLINDER

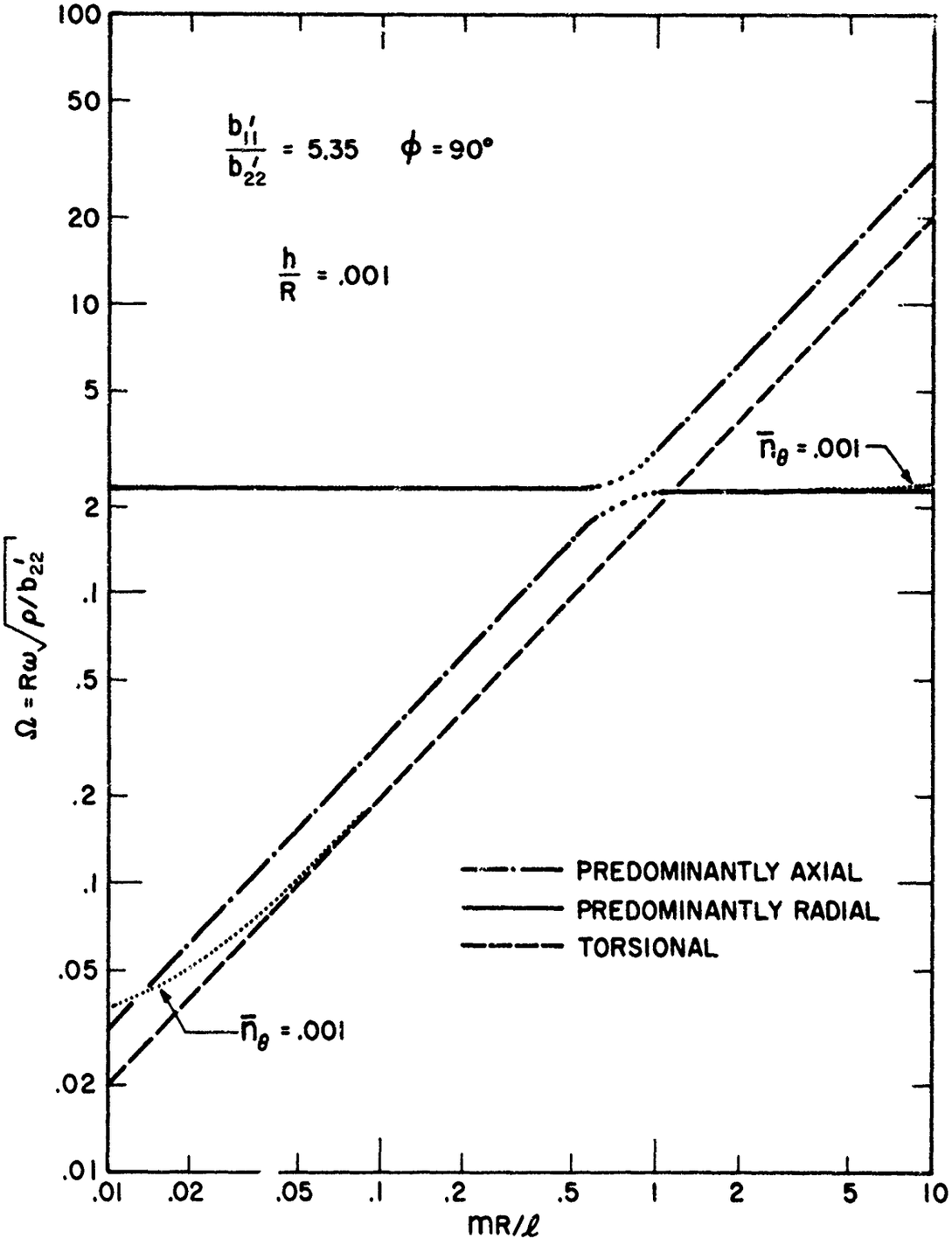

FIG. 5 FREQUENCY DISTRIBUTION OF n=0 MODE FOR CIRCUMFERENTIAL STIFFENING - CONSTANT THICKNESS ORTHOTROPIC CYLINDER

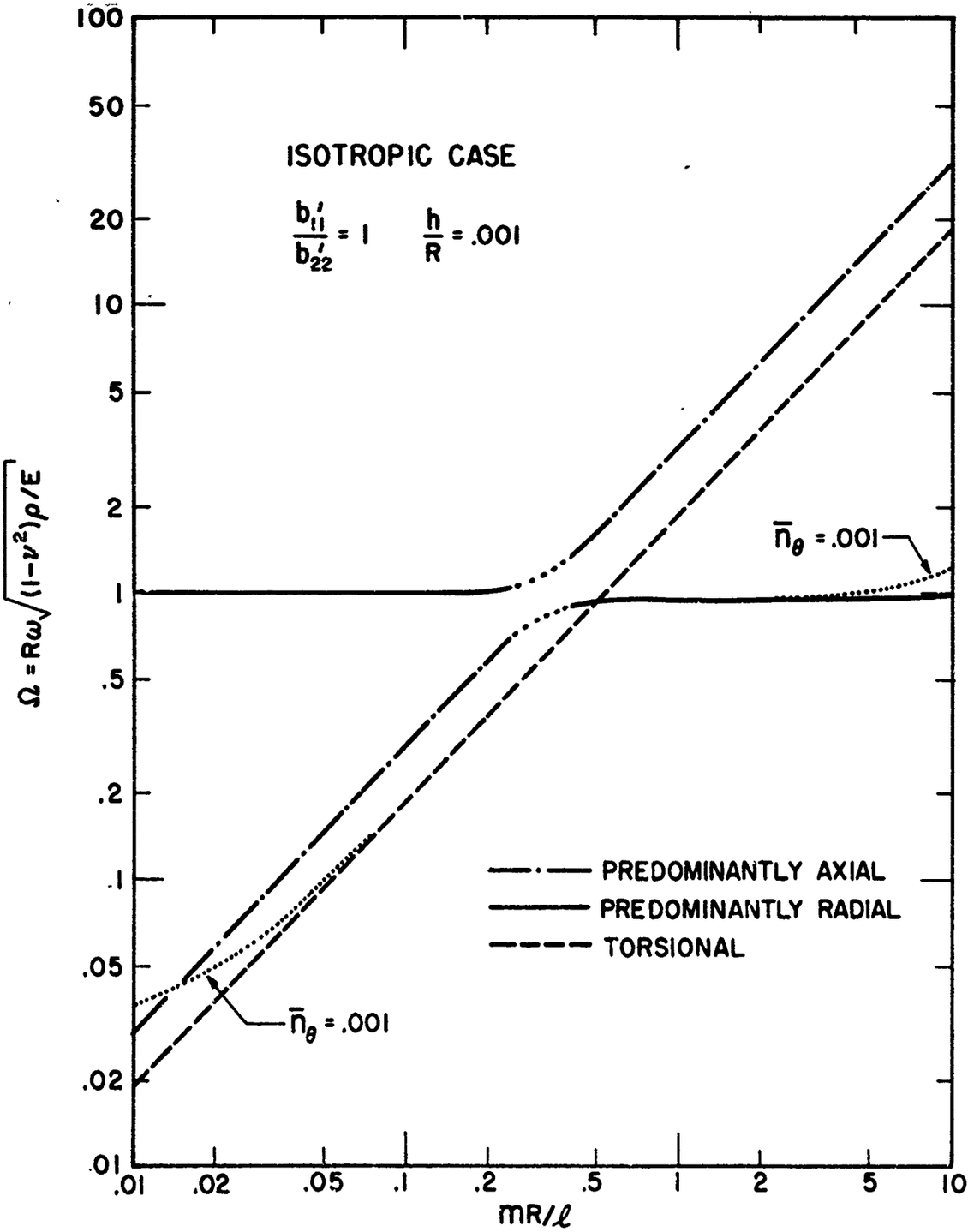

FIG. 6 FREQUENCY DISTRIBUTION OF n=0 MODE FOR ISOTROPIC CYLINDER

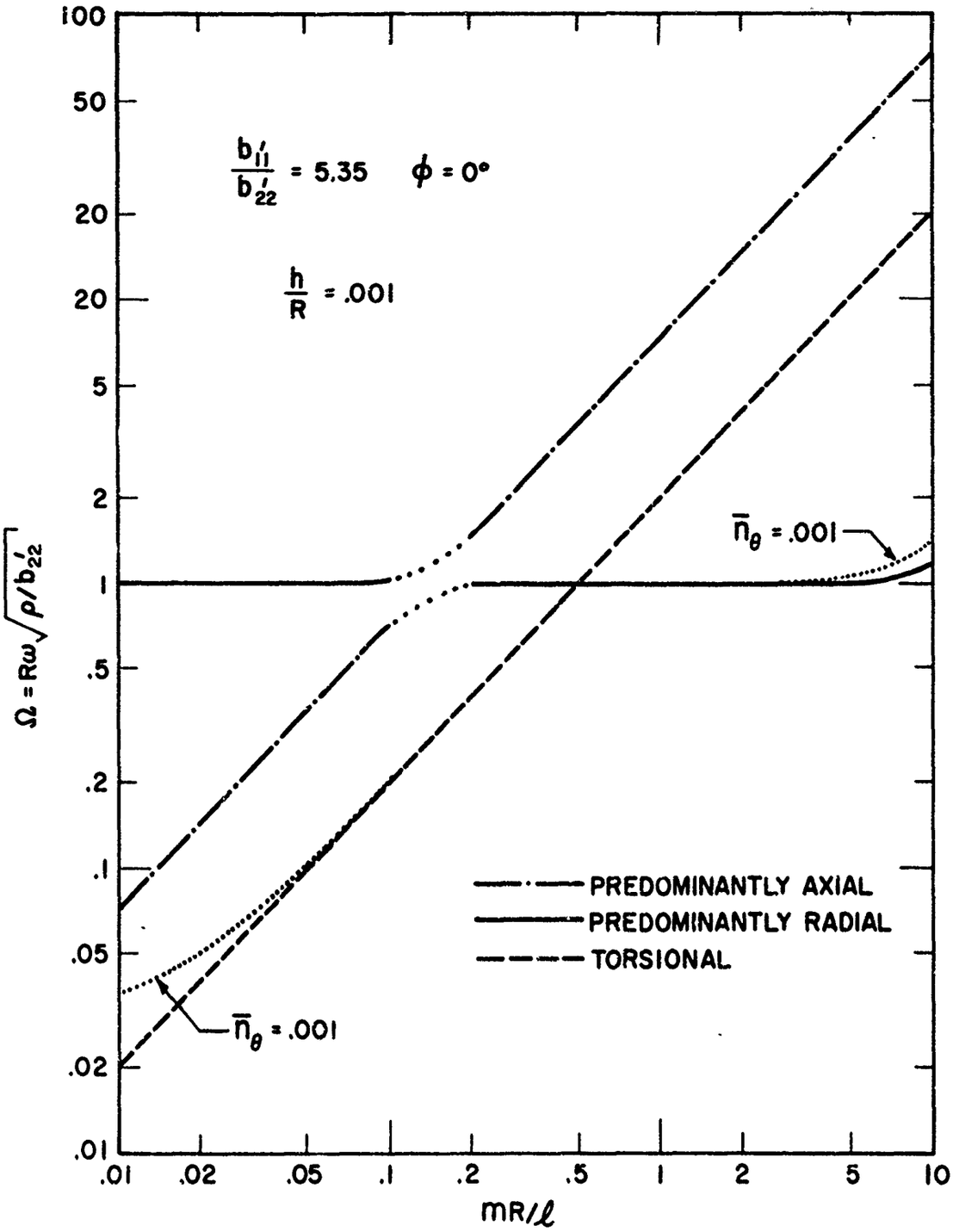

FIG. 7 FREQUENCY DISTRIBUTION OF n = 0 MODE FOR AXIAL STIFFENING – CONSTANT THICKNESS ORTHOTROPIC CYLINDER

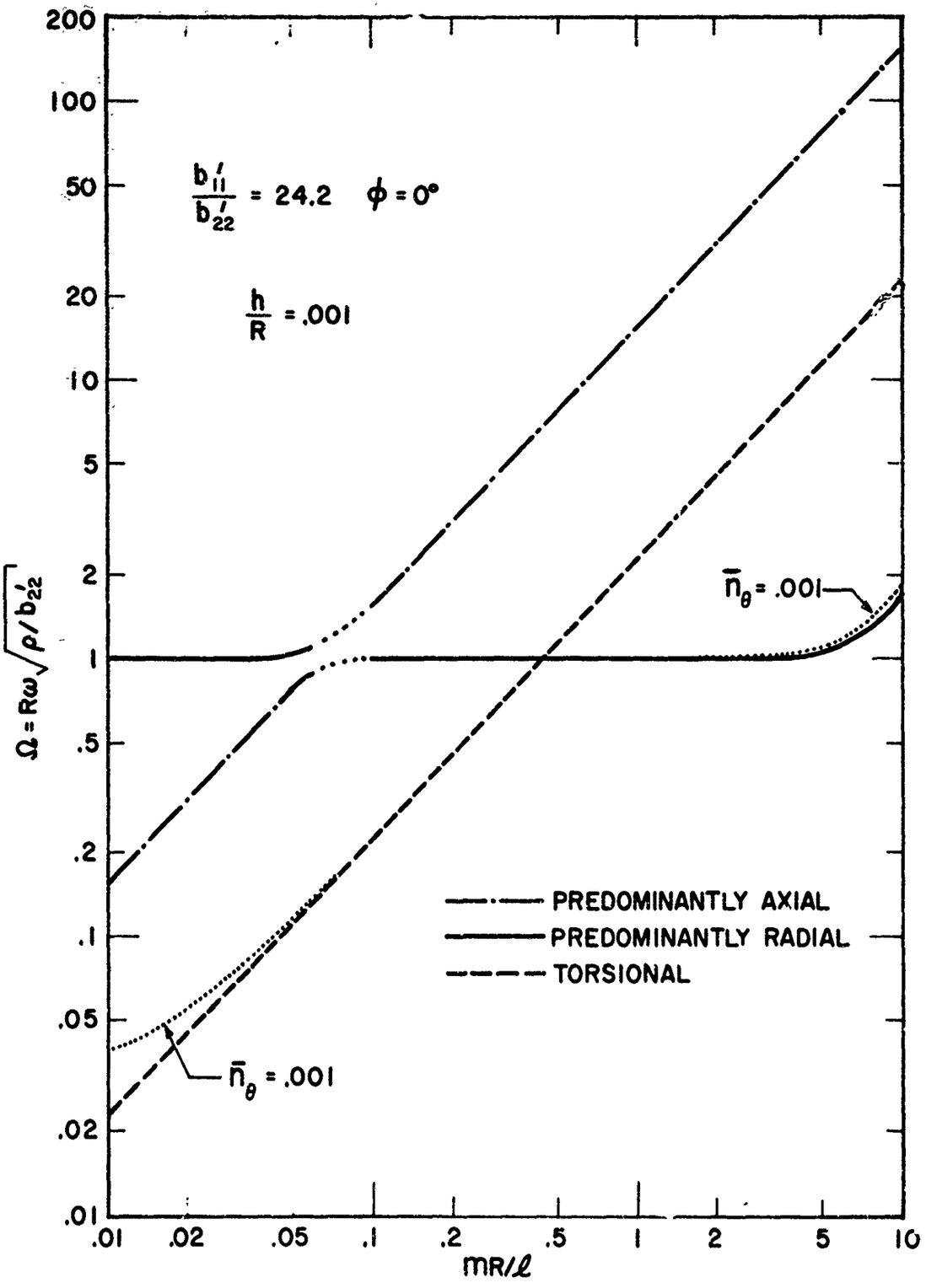

FIG. 8 FREQUENCY DISTRIBUTION OF n = 0 MODE FOR AXIAL STIFFENING - CONSTANT THICKNESS ORTHOTROPIC CYLINDER

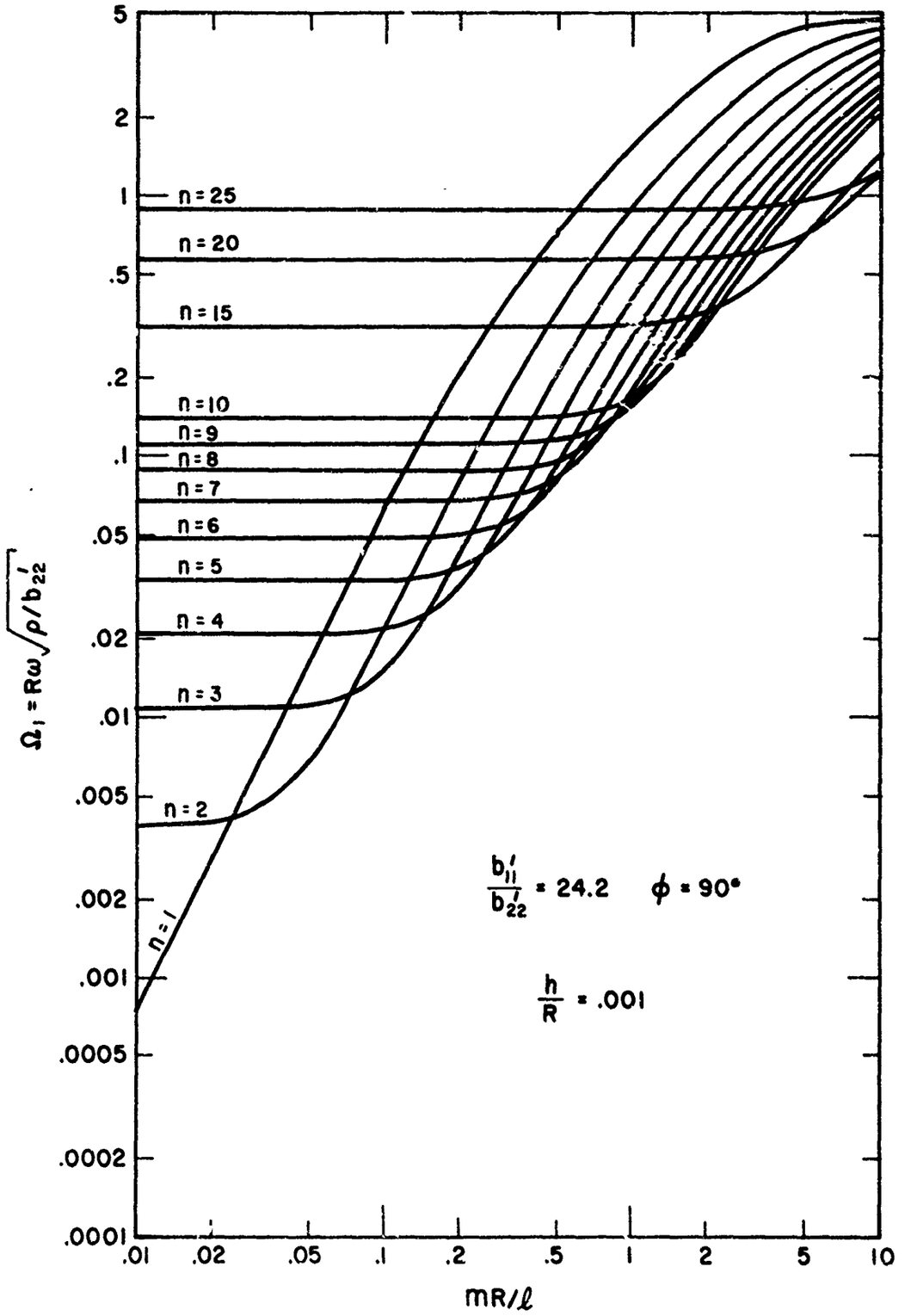

FIG. 9 FREQUENCIES OF $n \geq 1$ MODES FOR CIRCUMFERENTIAL STIFFENING-CONSTANT THICKNESS ORTHOTROPIC CYLINDER

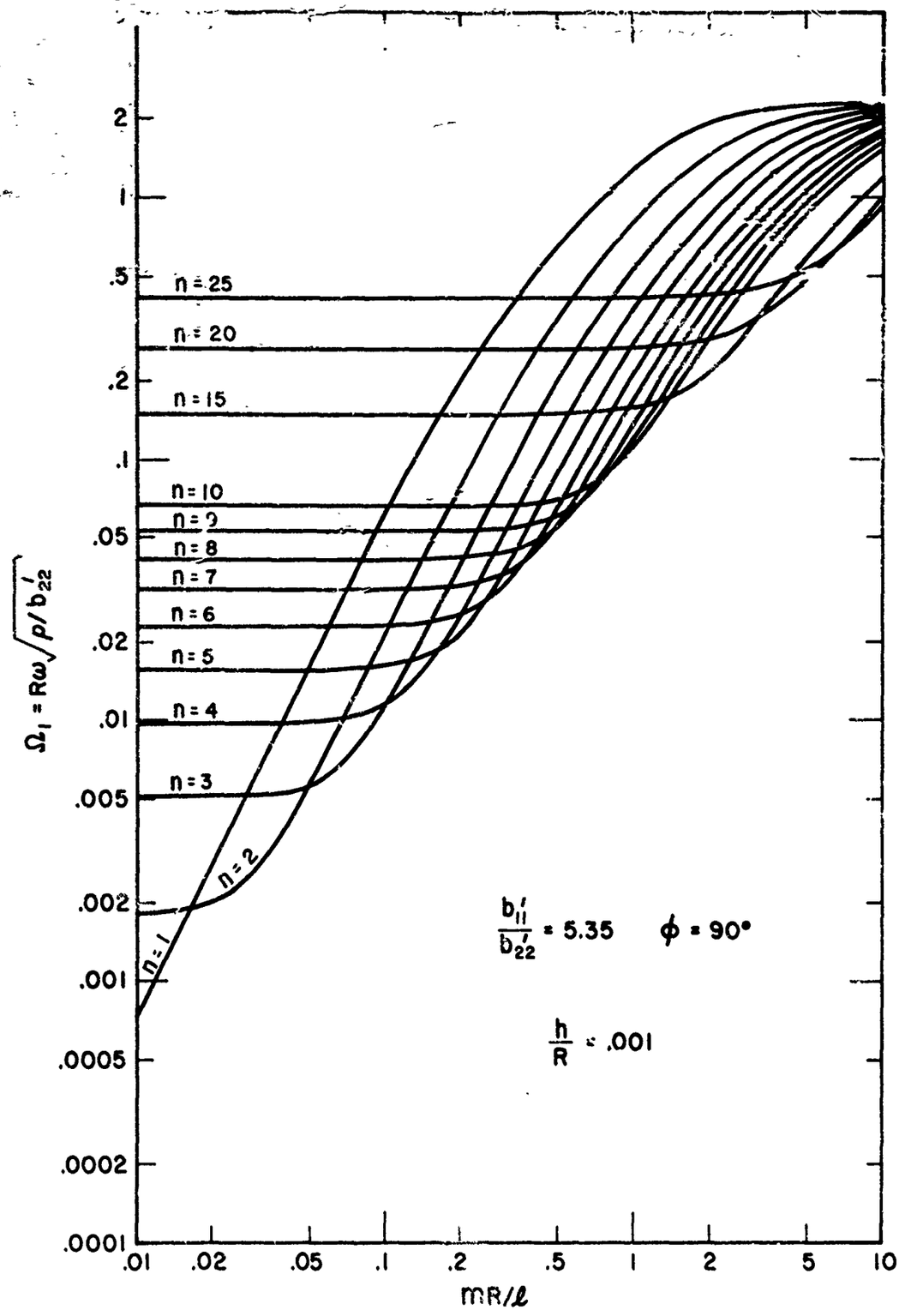

FIG. 10 FREQUENCIES OF $n \geq 1$ MODES FOR CIRCUMFERENTIAL STIFFENING - CONSTANT THICKNESS ORTHOTROPIC CYLINDER

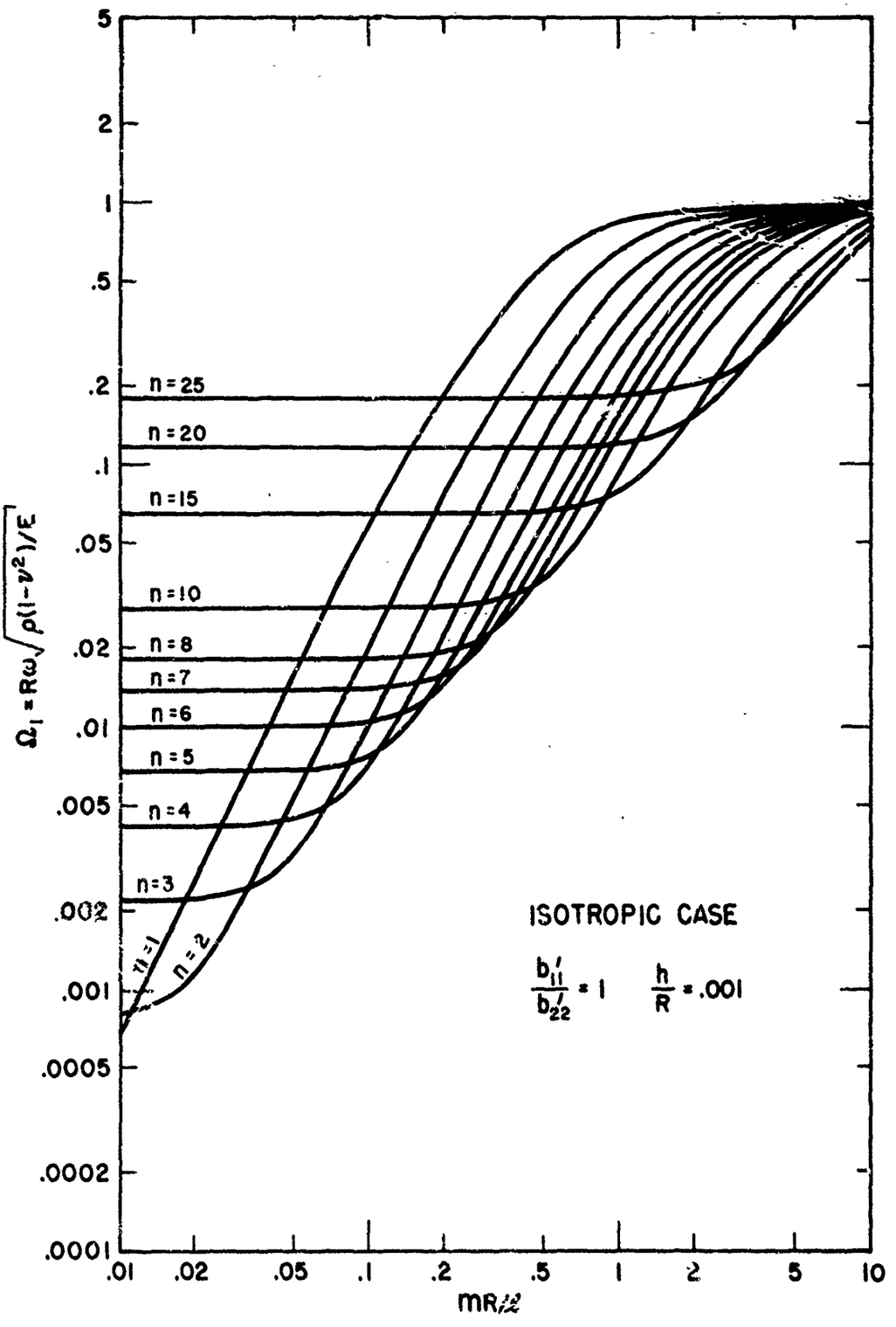

FIG. 11 FREQUENCIES OF $n \geq 1$ MODES FOR ISOTROPIC CYLINDER

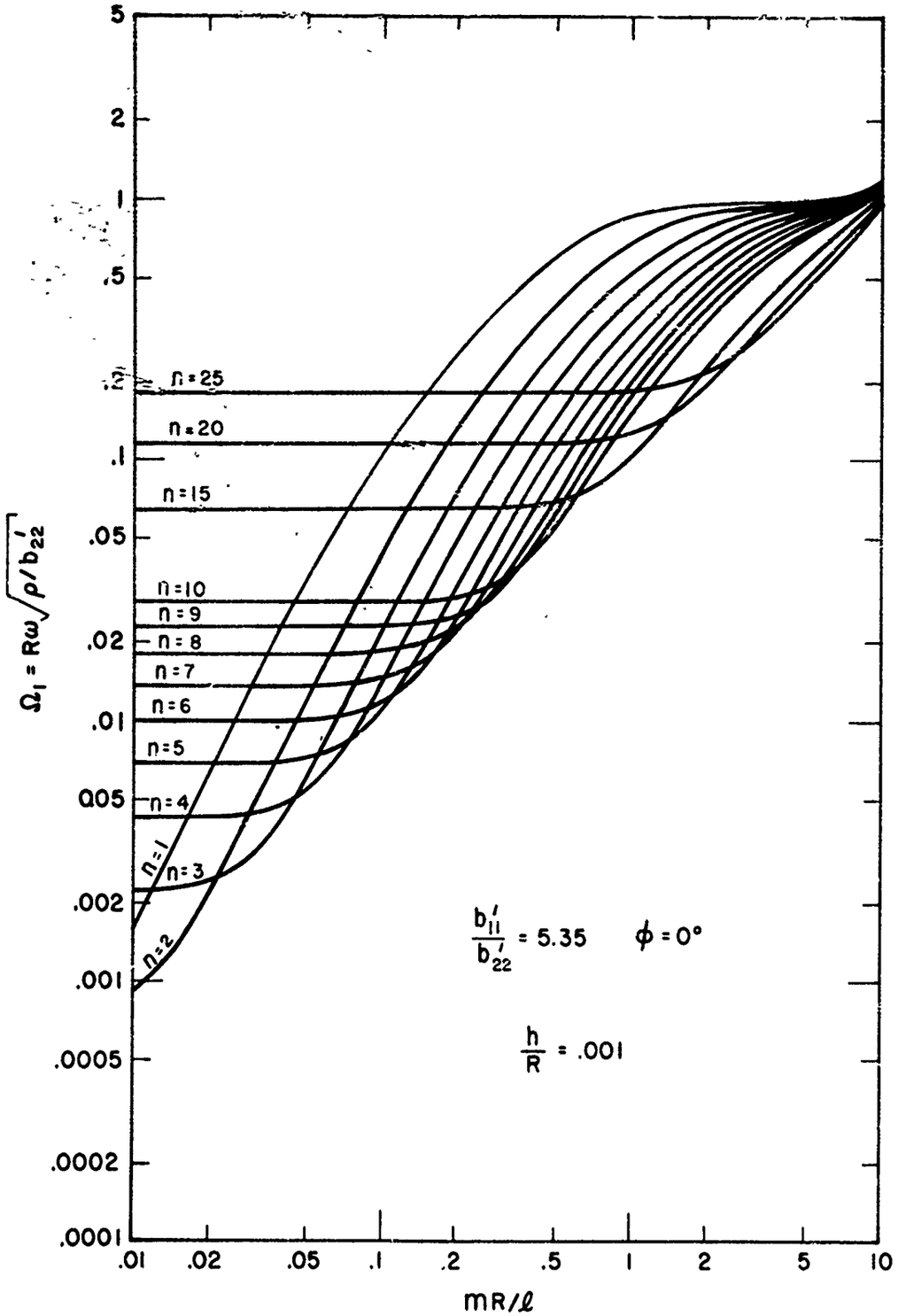

FIG. 12 FREQUENCIES OF $n \geq 1$ MODES FOR AXIAL STIFFENING - CONSTANT THICKNESS ORTHOTROPIC CYLINDER

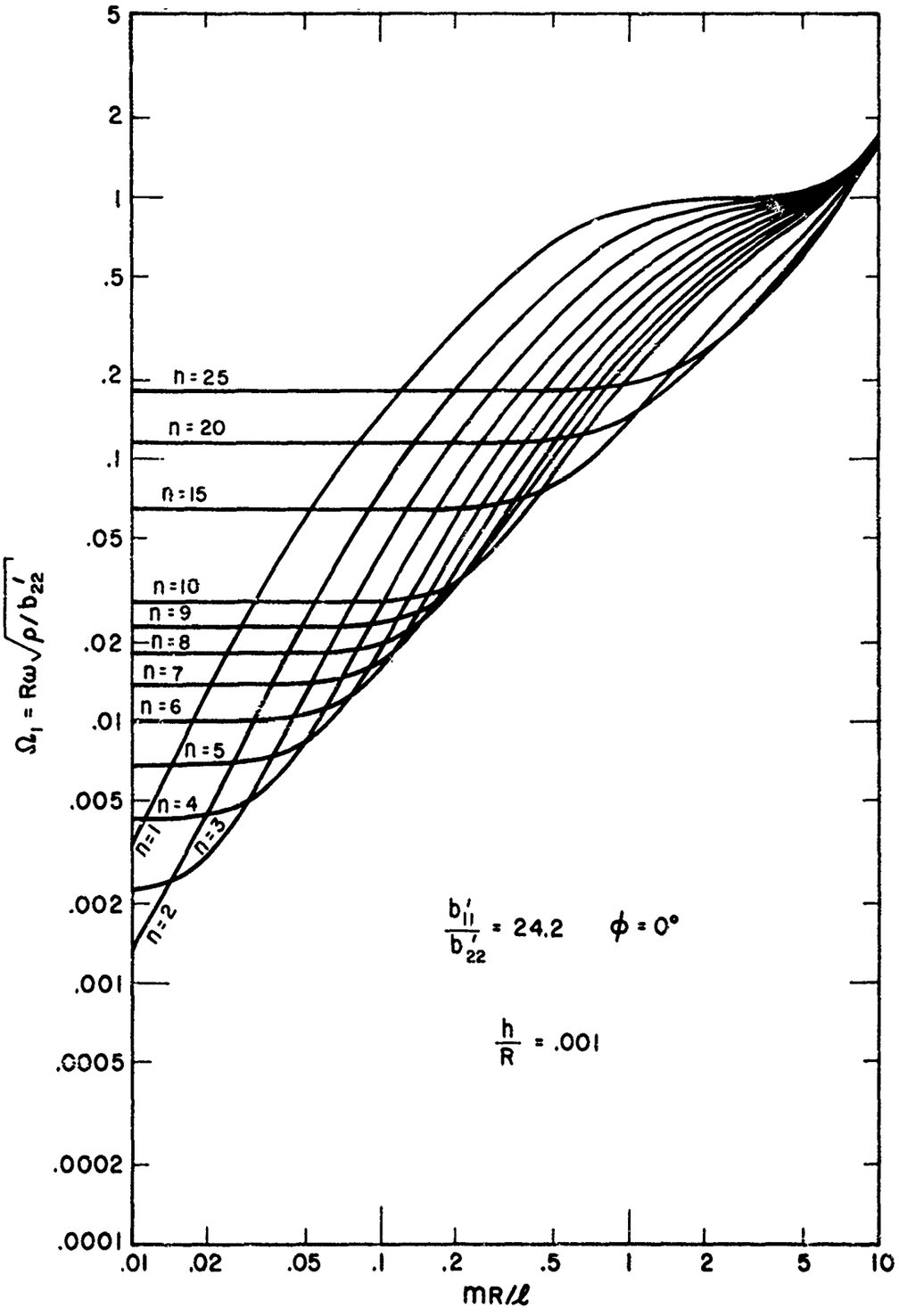

FIG. 13 FREQUENCIES OF $n \geq 1$ MODES FOR AXIAL STIFFENING – CONSTANT THICKNESS ORTHOTROPIC CYLINDER

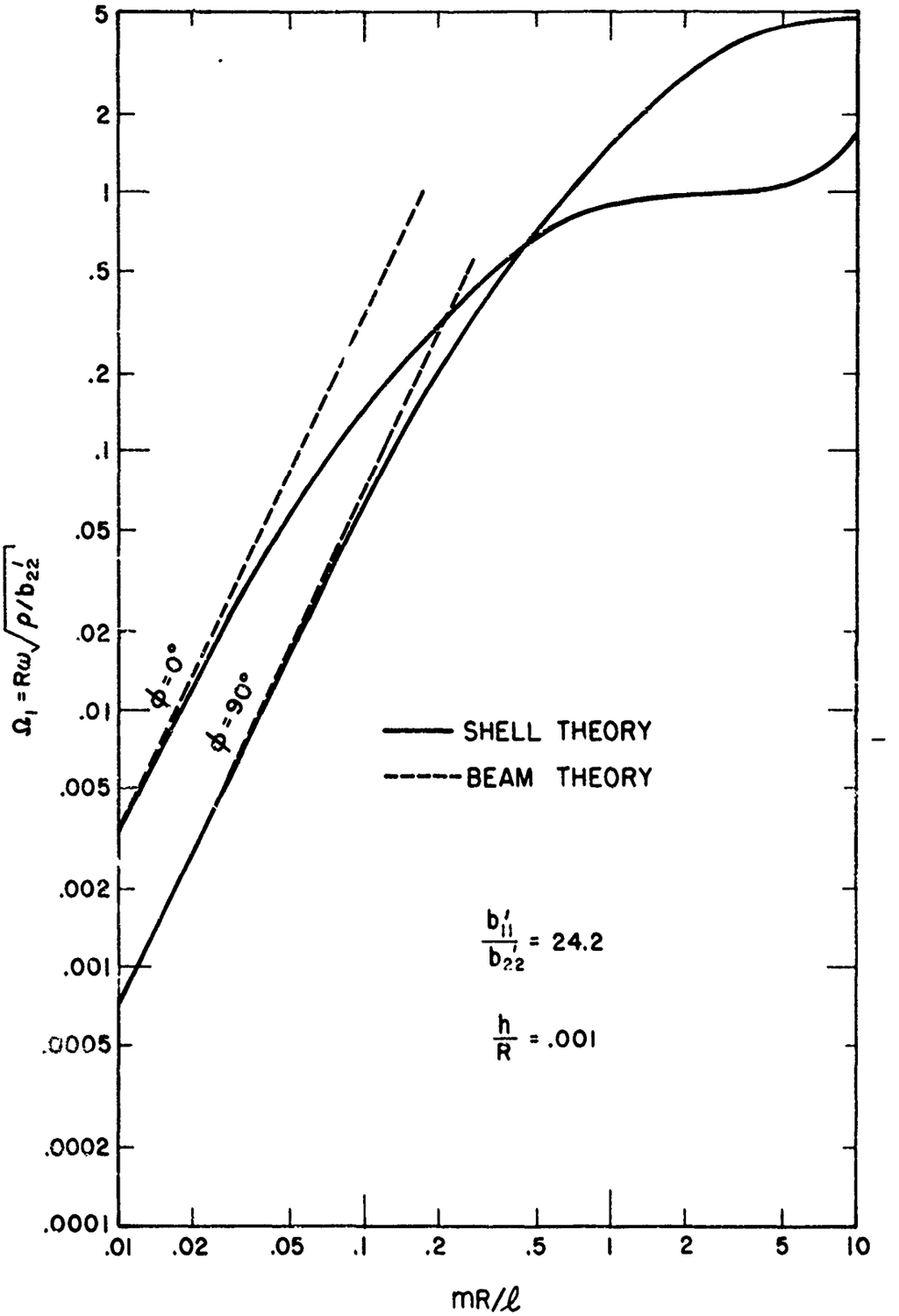

FIG. 14 FREQUENCIES OF THE BEAM TYPE MODE (n = 1) FOR CIRCUMFERENTIAL AND AXIAL STIFFENING

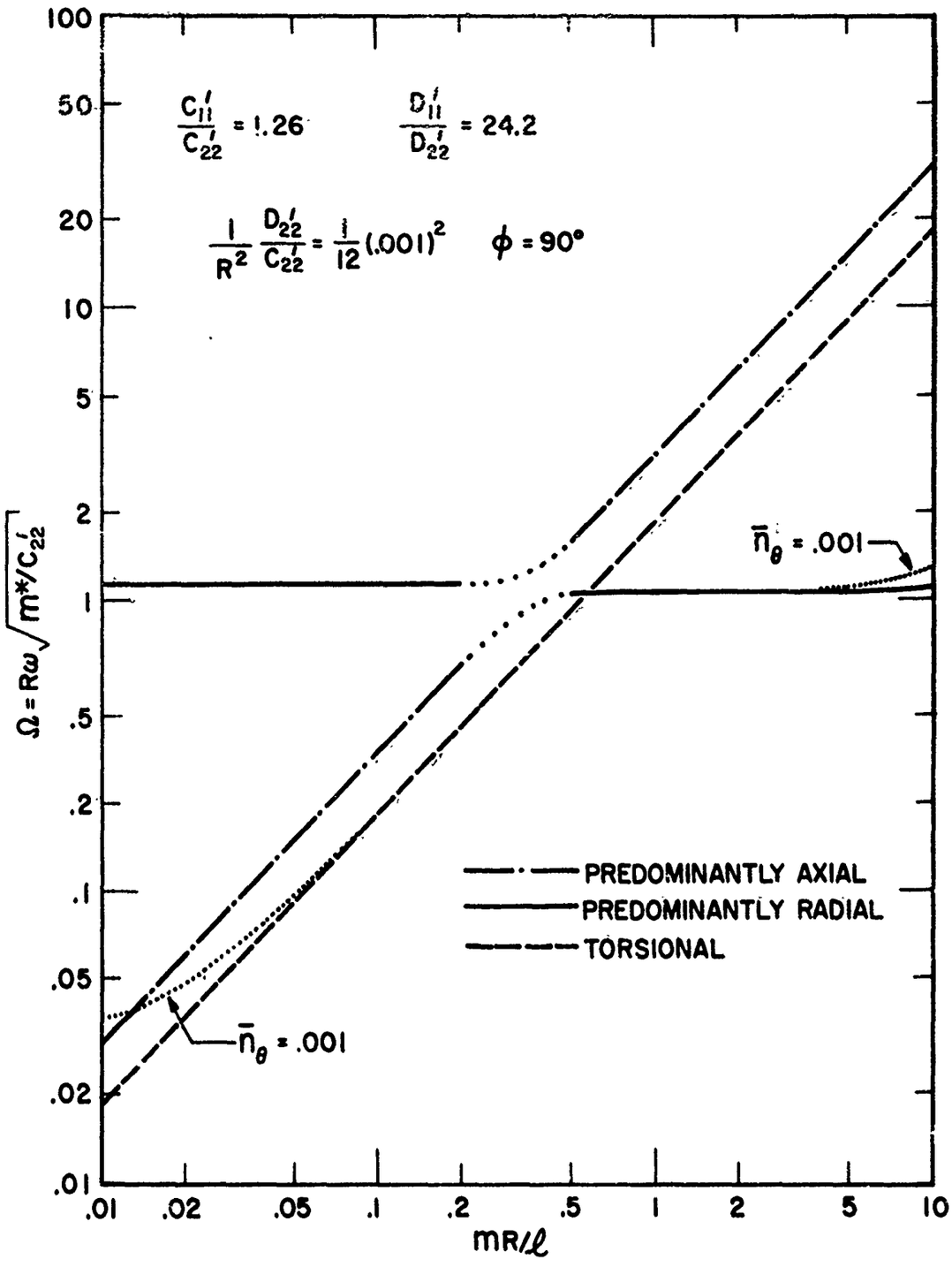

FIG. 15 FREQUENCY DISTRIBUTION OF n=0 MODE FOR CIRCUMFERENTIAL STIFFENING–STIFFENED CYLINDER

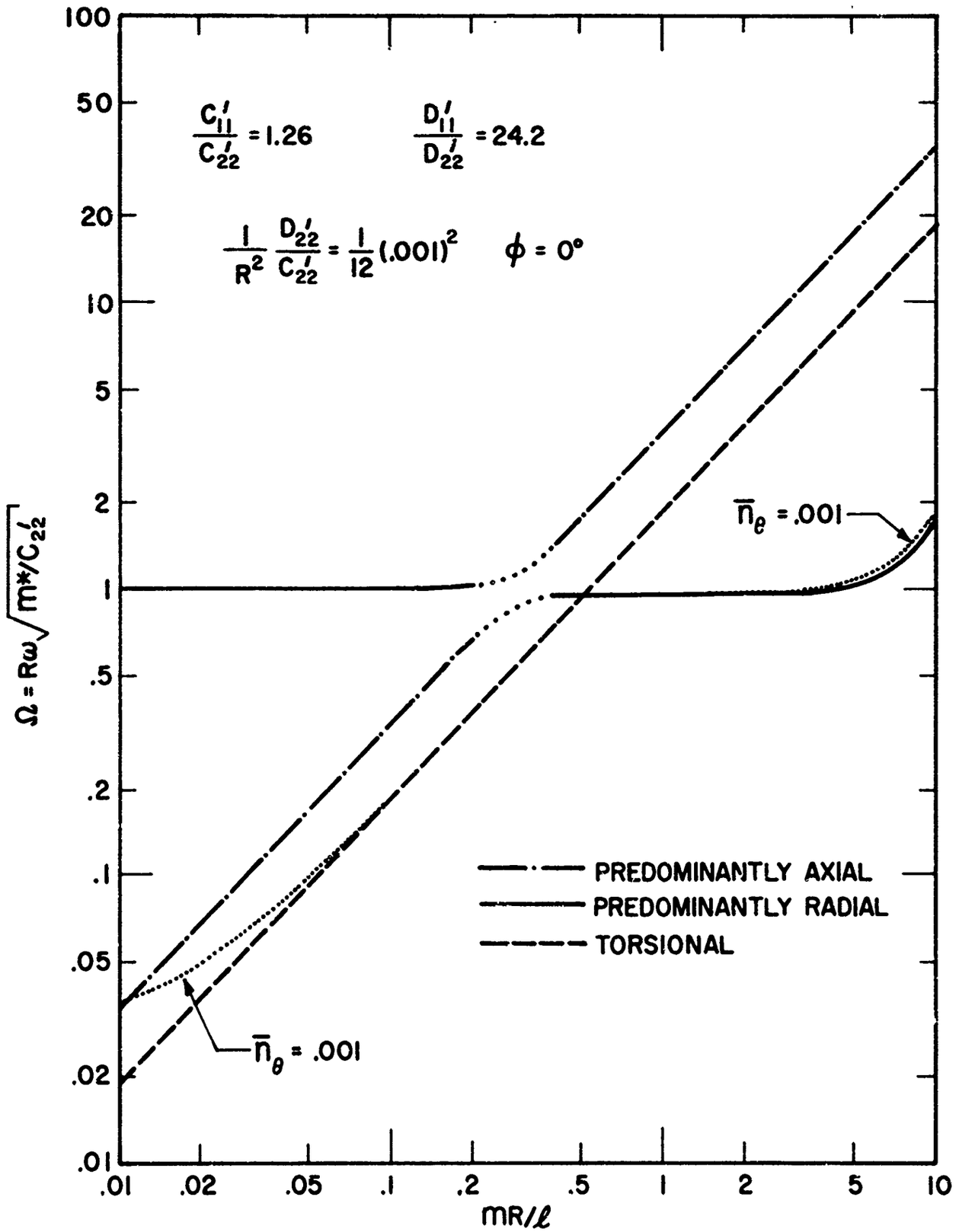

FIG. 16 FREQUENCY DISTRIBUTION OF n = 0 MODE FOR AXIAL STIFFENING - STIFFENED CYLINDER

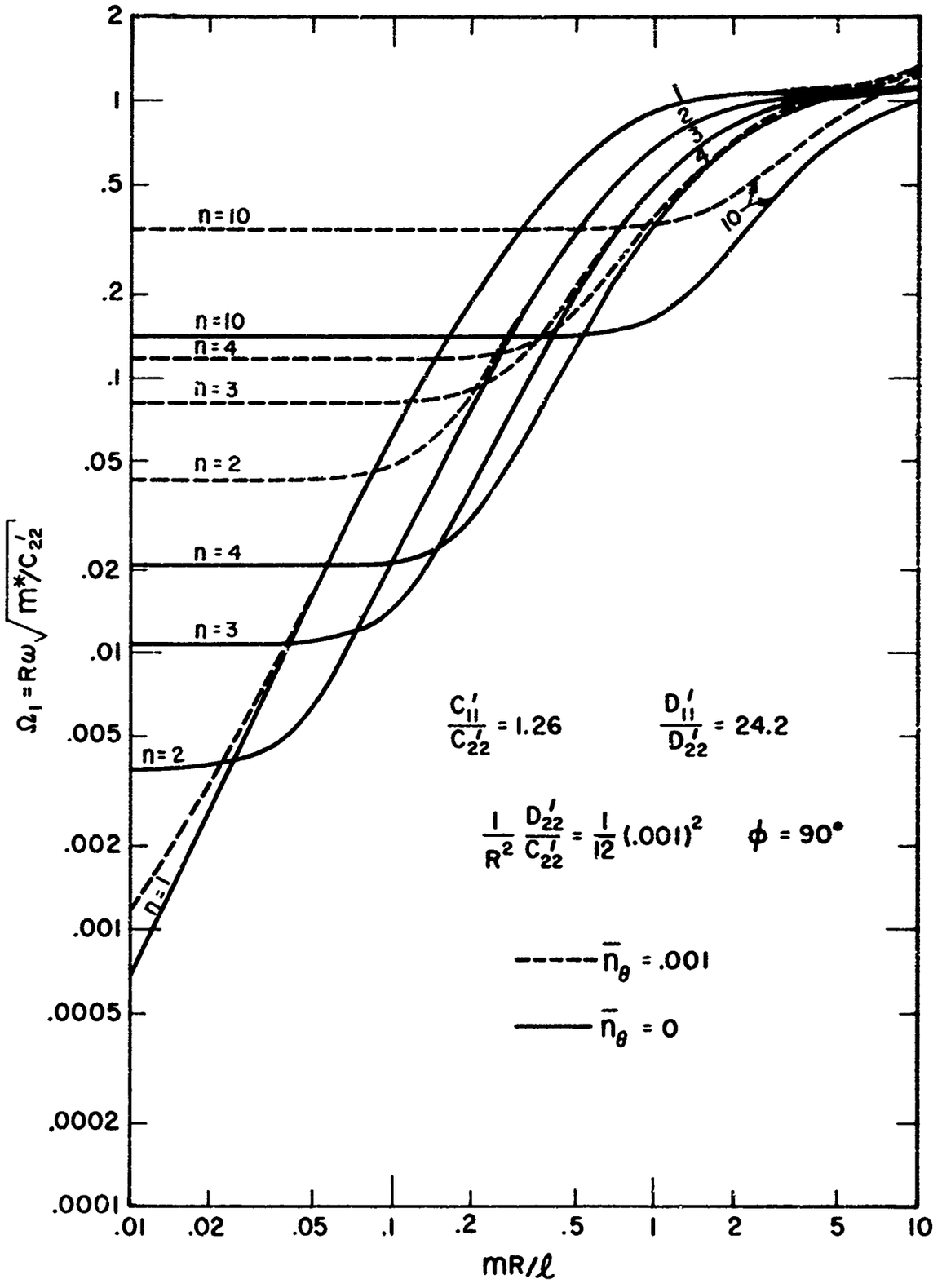

FIG. 17 FREQUENCIES OF $n \geq 1$ MODES FOR CIRCUMFERENTIAL STIFFENING - STIFFENED CYLINDER

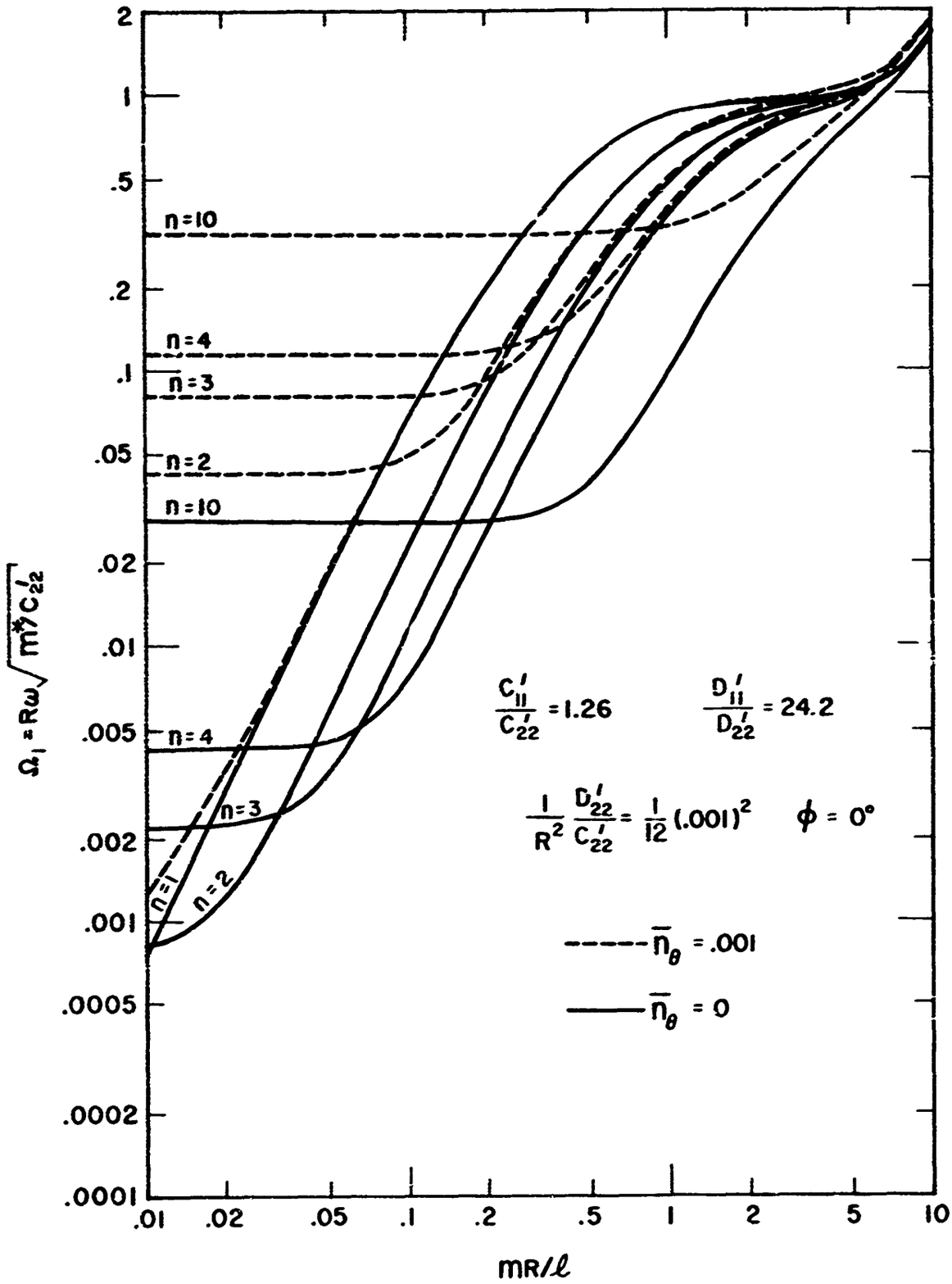

FIG. 18 FREQUENCIES OF $n \geq 1$ MODES FOR AXIAL STIFFENING - STIFFENED CYLINDER

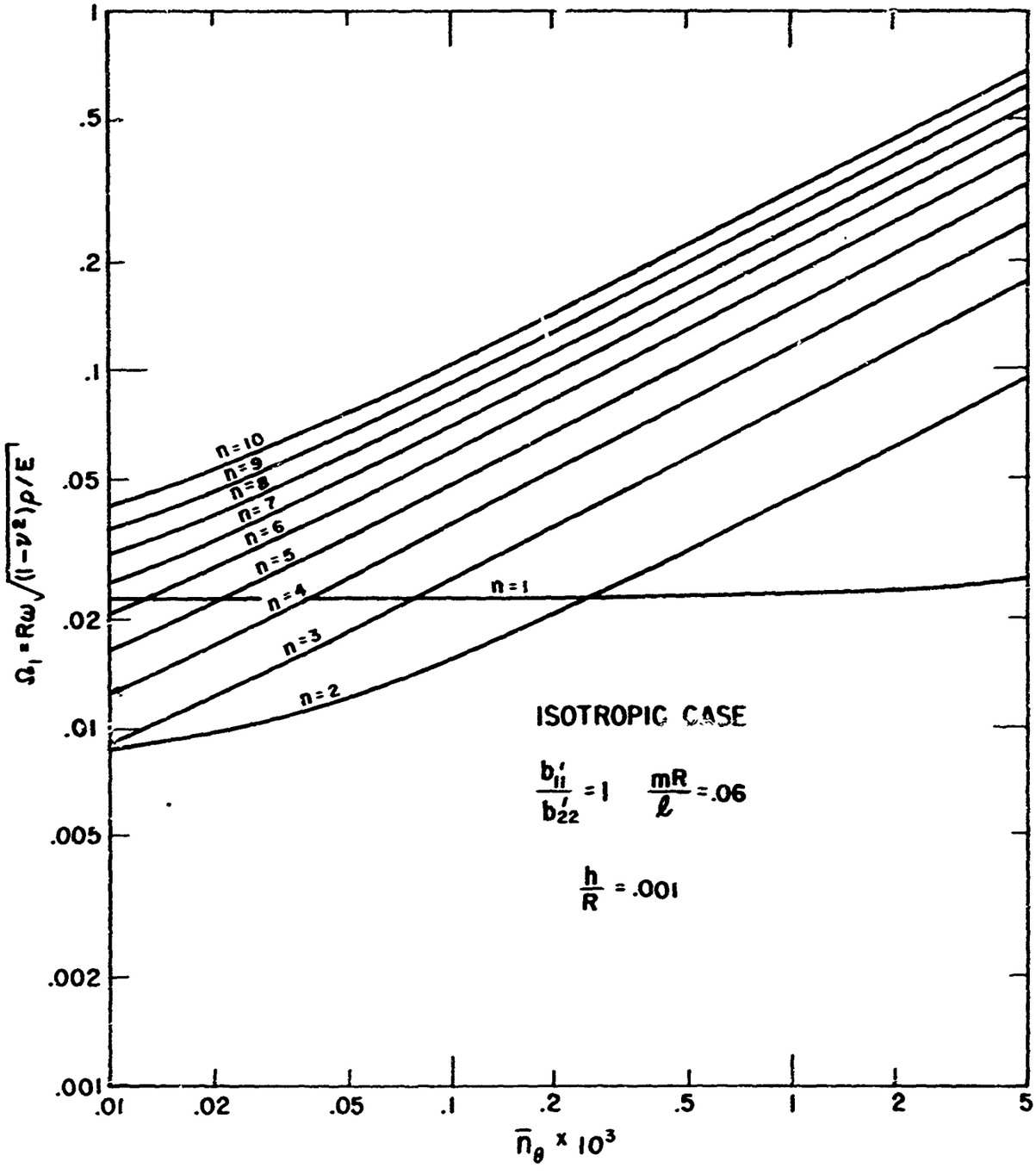

FIG. 19 VARIATION OF FREQUENCY WITH PRESSURE-STIFFNESS PARAMETER FOR VARIOUS CIRCUMFERENTIAL WAVE NUMBERS n – ISOTROPIC CYLINDER

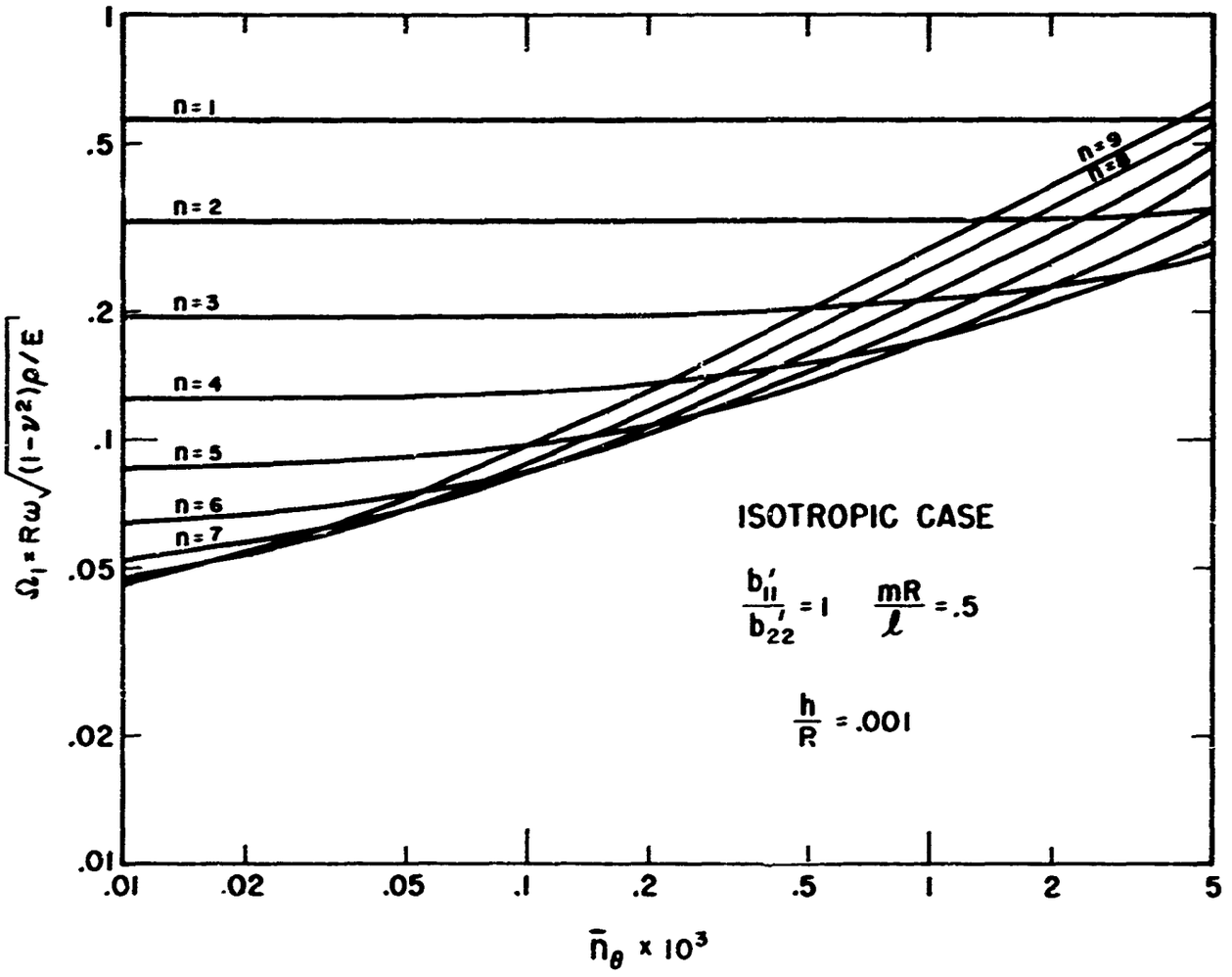

FIG. 20 VARIATION OF FREQUENCY WITH PRESSURE-STIFFNESS PARAMETER FOR VARIOUS CIRCUMFERENTIAL WAVE NUMBERS n – ISOTROPIC CYLINDER

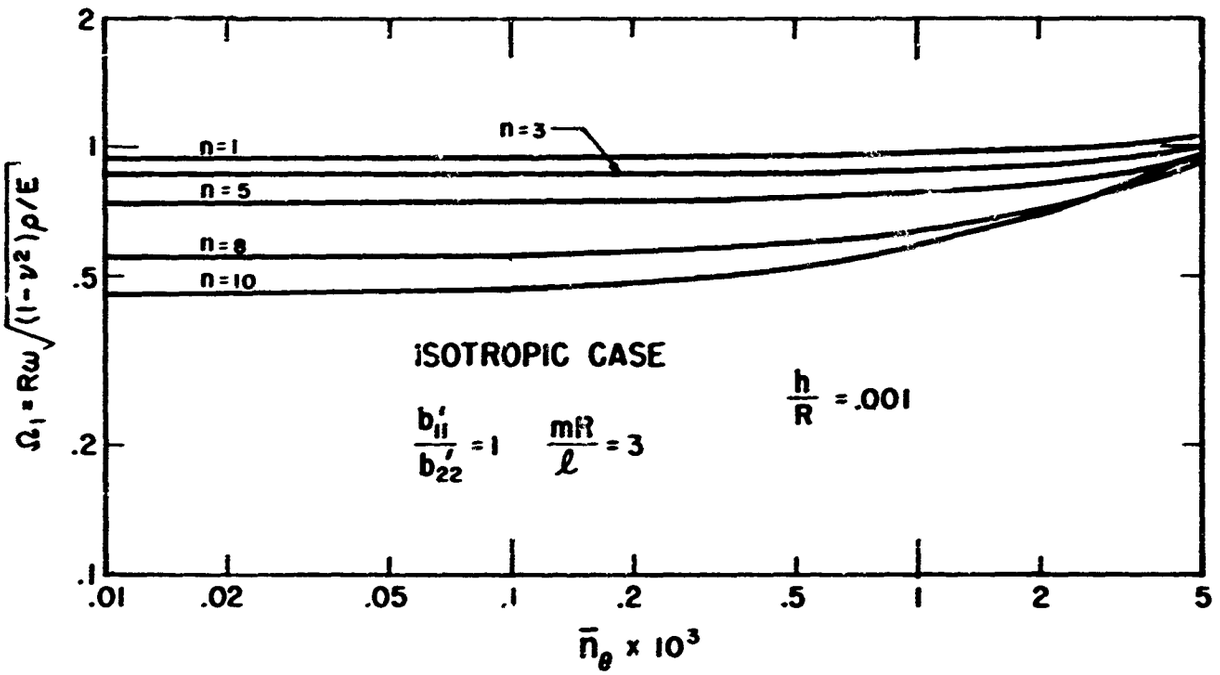

FIG. 21 VARIATION OF FREQUENCY WITH PRESSURE-STIFFNESS PARAMETER FOR VARIOUS CIRCUMFERENTIAL WAVE NUMBERS n—ISOTROPIC CYLINDER

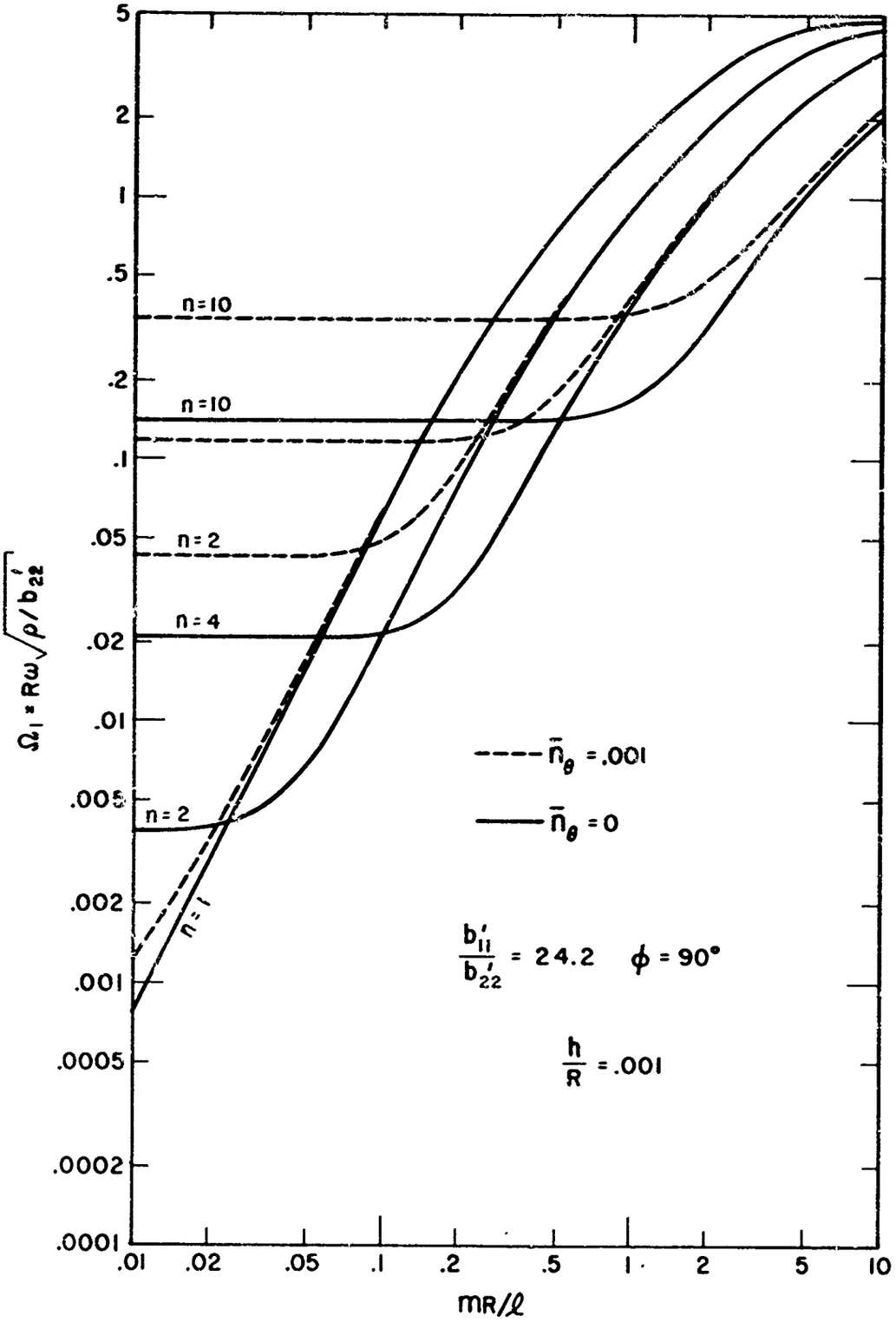

FIG. 22 EFFECT OF INTERNAL PRESSURE ON FREQUENCIES OF $n \geq 1$ MODES – CONSTANT THICKNESS ORTHOTROPIC CYLINDER

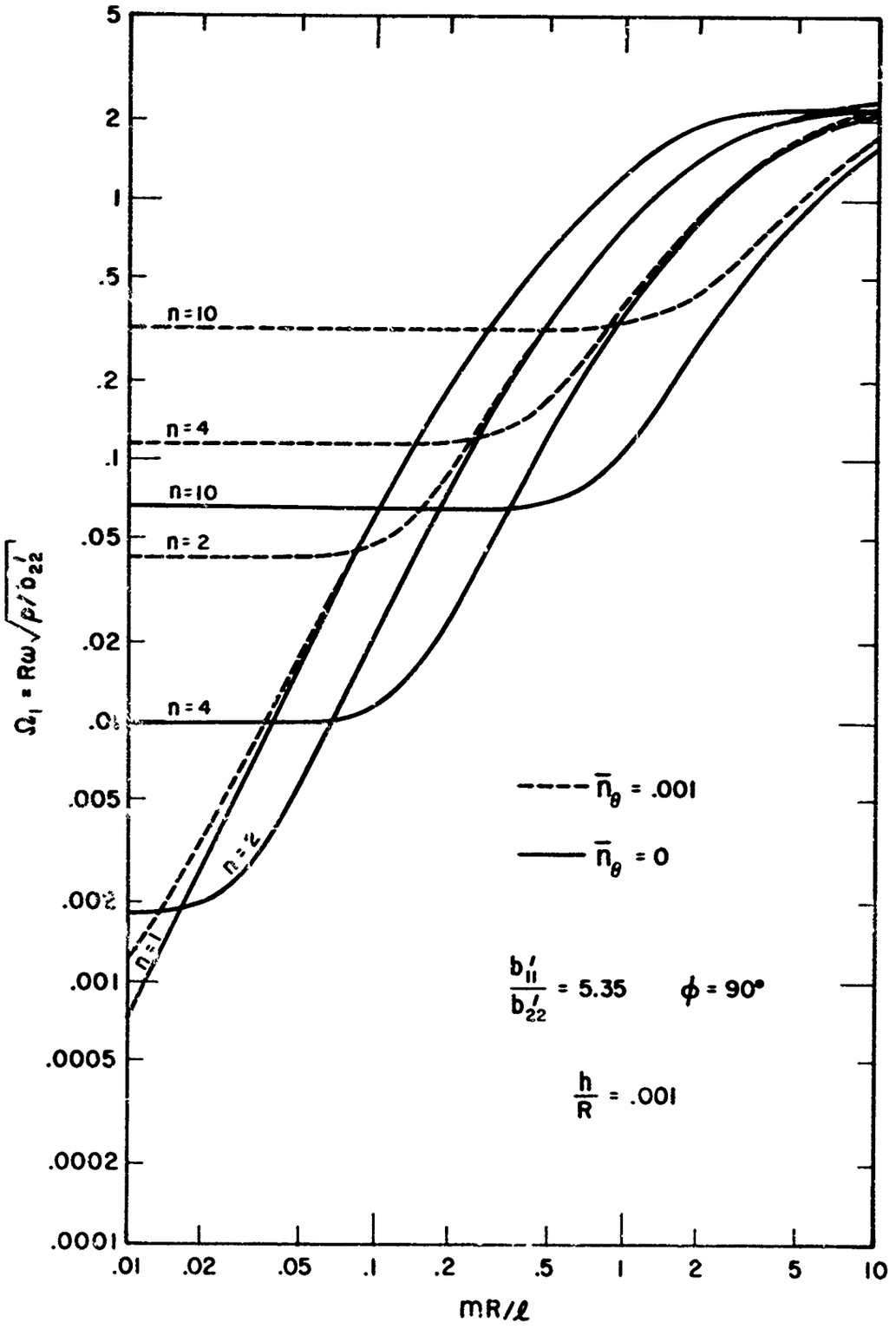

FIG. 23 EFFECT OF INTERNAL PRESSURE ON FREQUENCIES OF $n \geq 1$ MODES - CONSTANT THICKNESS ORTHOTROPIC CYLINDER

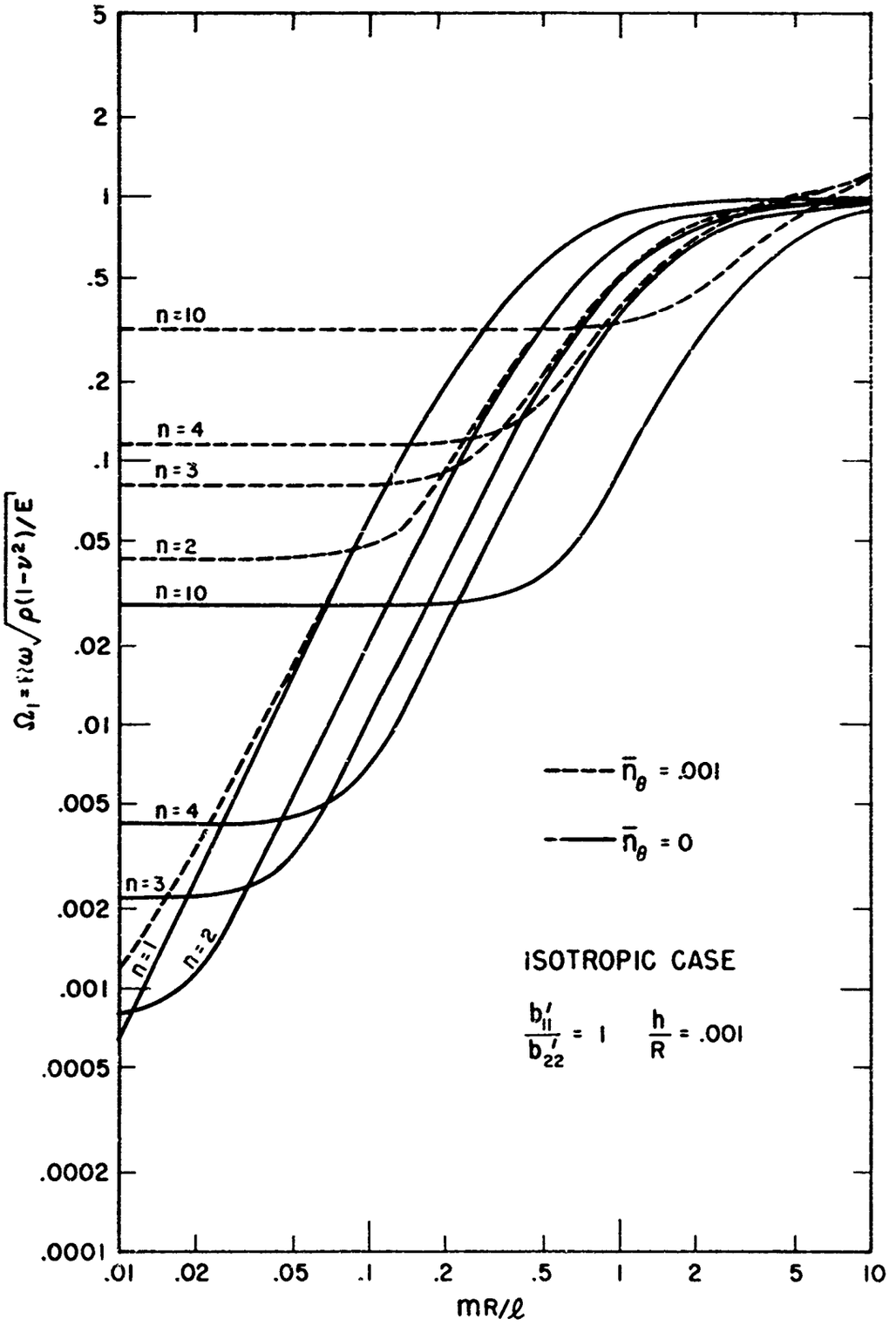

FIG. 24 EFFECT OF INTERNAL PRESSURE ON FREQUENCIES OF $n \geq 1$ MODES FOR ISOTROPIC CYLINDER

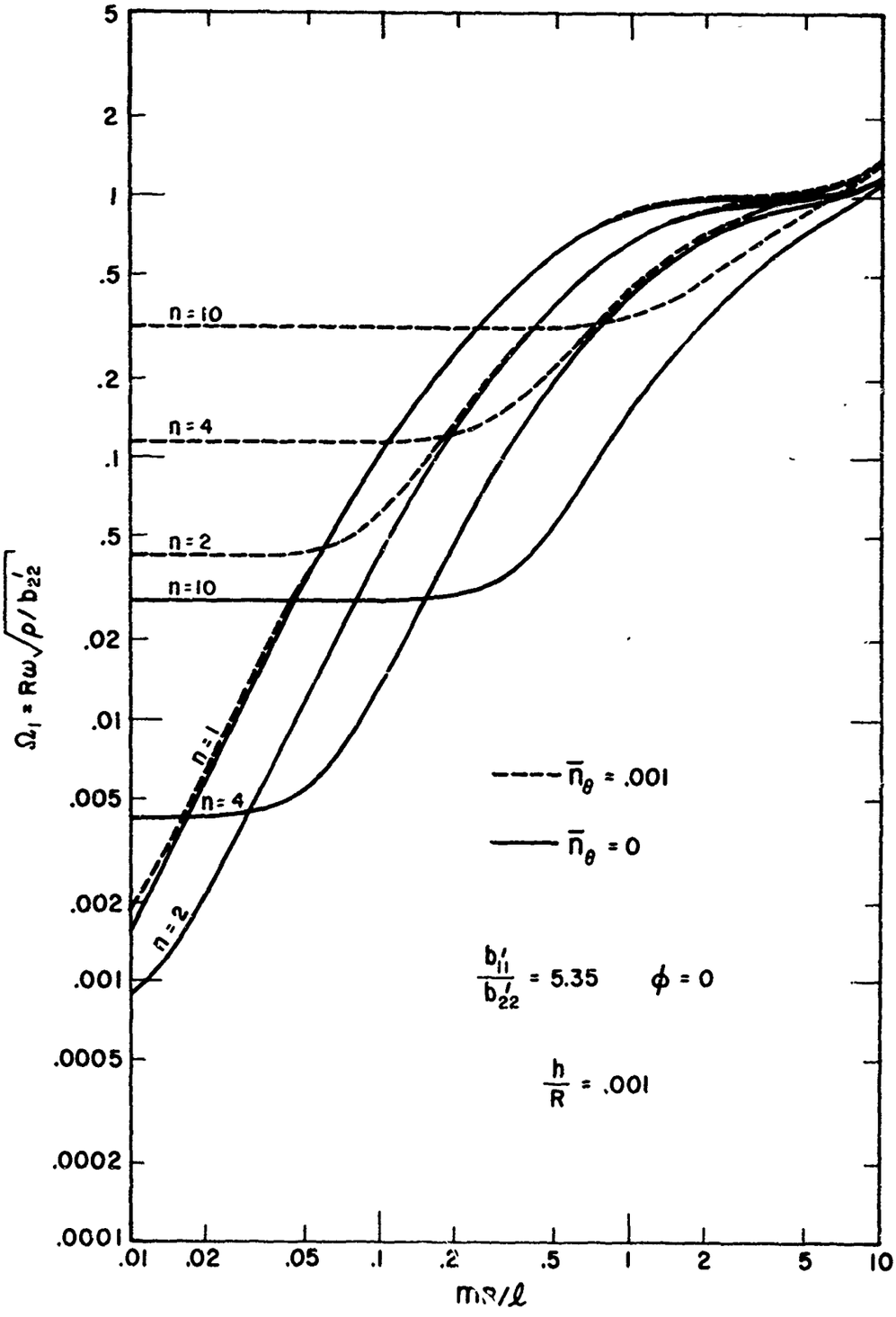

FIG. 25 EFFECT OF INTERNAL PRESSURE ON FREQUENCIES OF $n \geq 1$ MODES – CONSTANT THICKNESS ORTHOTROPIC CYLINDER

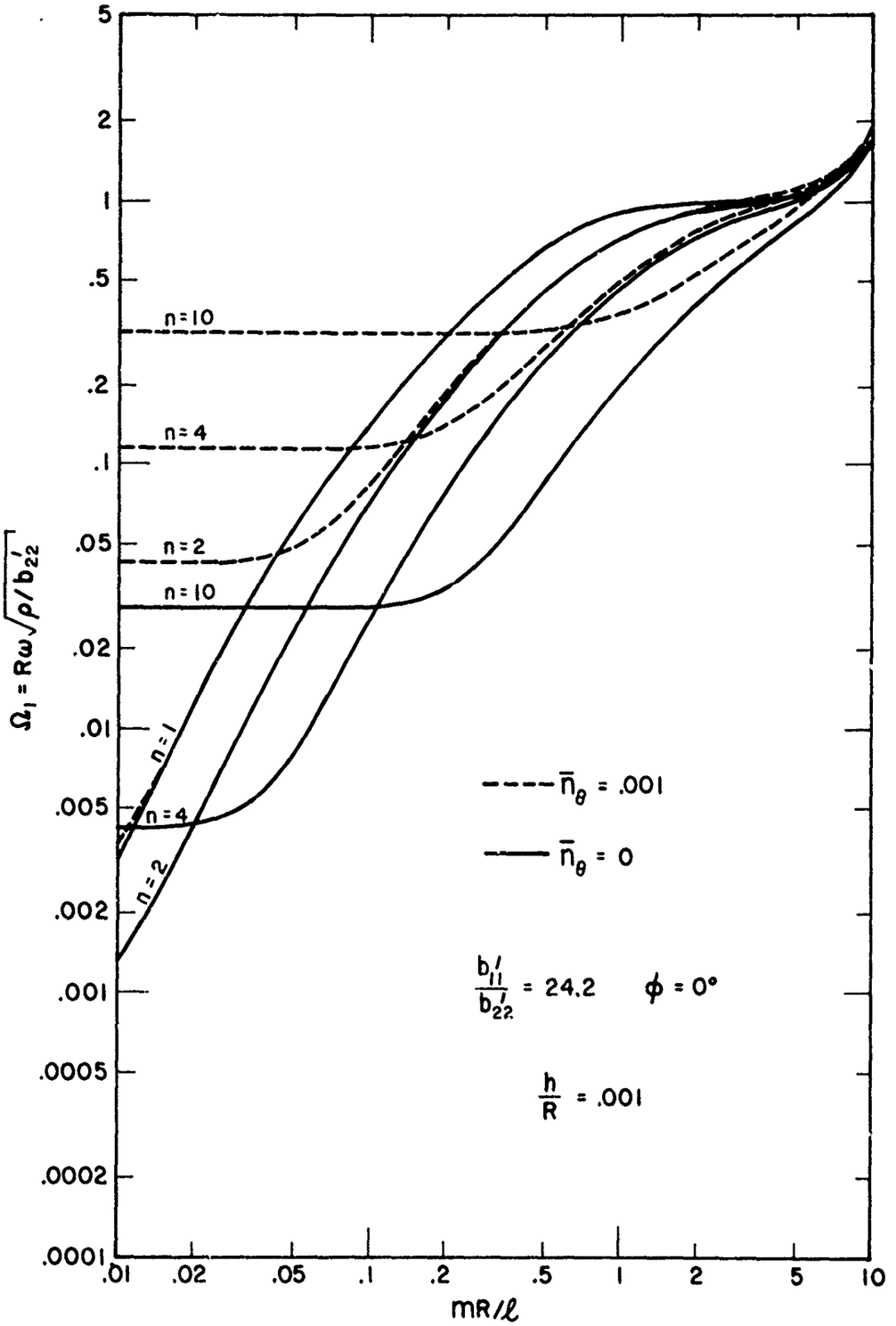

FIG. 26 EFFECT OF INTERNAL PRESSURE ON FREQUENCIES OF $n \geq 1$ MODES – CONSTANT THICKNESS ORTHOTROPIC CYLINDER